

BLENDING HIGH PERFORMANCE POLYMERS FOR IMPROVED STABILITY IN
INTEGRALLY SKINNED ASYMMETRIC GAS SEPARATION MEMBRANES

by

LESLIE SCHULTE

B.S., University of Kansas, 2010

AN ABSTRACT OF A DISSERTATION

submitted in partial fulfillment of the requirements for the degree

DOCTOR OF PHILOSOPHY

Department of Chemical Engineering
College of Engineering

KANSAS STATE UNIVERSITY
Manhattan, Kansas

2015

Abstract

Polyimide membranes have been used extensively in gas separation applications because of their attractive gas transport properties and the ease of processing these materials. Other applications of membranes, such as membrane reactors, which could compete with more traditional packed and slurry bed reactors across a wider range of environments, could benefit from improvements in the thermal and chemical stability of polymeric membranes. This work focuses on blending polyimide and polybenzimidazole polymers to improve the thermal and chemical stability of polyimide membranes while retaining the desirable characteristics of the polyimide.

Blended dense films and asymmetric membranes were fabricated and characterized. Dense film properties are useful for studying intrinsic properties of the polymer blends. Transport properties of dense films were characterized from room temperature to 200°C. Properties including miscibility, density, chain packing and thermal stability were investigated. A process for fabricating flat sheet blended integrally skinned asymmetric membranes by phase inversion was developed. The transport properties of membranes were characterized from room temperature to 300°C.

A critical characteristic of gas separation membranes is selectivity. Post-treatments including thermal annealing and vapor and liquid surface treatments were investigated to improve the selectivity of blended membranes. Vapor and liquid surface treatments with common, benign solvents including an alkane, an aldehyde and an alcohol resulted in improvements in selectivity.

BLENDING HIGH PERFORMANCE POLYMERS FOR IMPROVED STABILITY IN
INTEGRALLY SKINNED ASYMMETRIC MEMBRANES

by

LESLIE SCHULTE

B.S., University of Kansas, 2010

A DISSERTATION

submitted in partial fulfillment of the requirements for the degree

DOCTOR OF PHILOSOPHY

Department of Chemical Engineering
College of Engineering

KANSAS STATE UNIVERSITY
Manhattan, Kansas

2015

Approved by:

Major Professor
Mary E. Rezac

Abstract

Polyimide membranes have been used extensively in gas separation applications because of their attractive gas transport properties and the ease of processing these materials. Other applications of membranes, such as membrane reactors, which could compete with more traditional packed and slurry bed reactors across a wider range of environments, could benefit from improvements in the thermal and chemical stability of polymeric membranes. This work focuses on blending polyimide and polybenzimidazole polymers to improve the thermal and chemical stability of polyimide membranes while retaining the desirable characteristics of the polyimide.

Blended dense films and asymmetric membranes were fabricated and characterized. Dense film properties are useful for studying intrinsic properties of the polymer blends. Transport properties of dense films were characterized from room temperature to 200°C. Properties including miscibility, density, chain packing and thermal stability were investigated. A process for fabricating flat sheet blended integrally skinned asymmetric membranes by phase inversion was developed. The transport properties of membranes were characterized from room temperature to 300°C.

A critical characteristic of gas separation membranes is selectivity. Post-treatments including thermal annealing and vapor and liquid surface treatments were investigated to improve the selectivity of blended membranes. Vapor and liquid surface treatments with common, benign solvents including an alkane, an aldehyde and an alcohol resulted in improvements in selectivity.

Table of Contents

List of Figures	viii
List of Tables	xii
Acknowledgements	xiii
Dedication	xiv
Chapter 1 - Introduction	1
Chapter 2 - Background and theory	7
1. Transport theory	7
2. Phase inversion	11
3. Behavior of blends of polymers	12
Chapter 3 - Blended PBI/Matrimid films and asymmetric membranes; Fabrication and characterization	14
1. Introduction	14
2. Experimental	17
2.1. Materials	17
2.2 Preparation of dense films	17
2.2.1 Preparation of Matrimid films	17
2.2.2 Preparation of blend and PBI films	17
2.3 Cloud point measurements	18
2.4 Preparation of asymmetric membranes	18
2.4.1 Fabrication of Matrimid membranes	18
2.4.2 Fabrication of PBI-Matrimid membranes	19
2.5 Characterization methods	19
2.5.1 Gas transport	19
2.5.2 Density	20
2.5.3 Miscibility	20
2.5.4 Morphology	20
2.5.5 Chain packing	20
2.5.6 Thermal and chemical stability	20

3. Results and discussion	21
3.1. Appearance of dense films and asymmetric membranes	21
3.2. Miscibility of dense films	23
3.3. Gas transport properties of dense films	23
3.4. Cloud point diagrams	26
3.5. Optimizing membrane fabrication procedures for asymmetric membranes: Comments, and the importance of coagulation bath temperature and evaporation time on gas transport properties.....	29
3.6. Characterizing 50/50 asymmetric blend membranes	32
4. Conclusions.....	34
Chapter 4 - Thermal stability of PBI/Matrimid films and membranes	35
1. Introduction.....	35
2. Experimental.....	37
2.1 Materials	37
2.2 Dense films and asymmetric membranes	37
2.3 Characterization methods.....	38
2.3.1 Gas transport measurements	38
2.3.2 Chain packing	38
2.3.3 Thermal stability	38
3. Results and discussion	38
3.1 Dense blend PBI/Matrimid films	38
3.2 50/50 PBI/Matrimid asymmetric membranes	40
3.2.1 Stability of 50/50 PBI/Matrimid at 200°C.....	42
3.2.2 Stability of 50/50 PBI/Matrimid at 300°C.....	46
3.2.3 Properties of 50/50 PBI/Matrimid membranes annealed at 200°C.....	47
4. Conclusions.....	48
Chapter 5 - Mild solvent post treatments of blended asymmetric PBI/Matrimid membranes	50
1. Introduction.....	50
2. Experimental.....	51
2.1. Materials	51
2.2 Fabrication of asymmetric PBI-Matrimid membranes	51

2.3 Vapor post-treatments of asymmetric PBI-Matrimid membranes	51
2.4 Liquid post-treatments of asymmetric PBI-Matrimid membranes	51
2.5 Measuring transport properties	52
2.6 Data analysis	52
3. Results and discussion	52
3.1 Selection of treatments.....	52
3.2 Vapor post-treatments.....	54
3.3 Liquid post-treatments	59
4. Conclusions.....	61
Chapter 6 - Conclusions and future work	62
References.....	64
Appendix A - Dynamic Mechanical Analysis Data.....	72

List of Figures

Figure 1–1. A membrane controls the transport of molecules through it. The feed consists of two components A and B. Because component B passes through the membrane more readily, the permeate will be enriched in component B.....	1
Figure 1–2. A model Loeb-Sourirajan membrane with a thin, dense selective skin layer which controls the separation. In this region, the gas meets most of the resistance to mass transfer. The bulk of the membrane thickness is a porous substructure that serves as a support for the skin layer. In this region, the gas meets little to no resistance.....	3
Figure 1–3. Schematic of a membrane reactor as a phase contactor	4
Figure 2–1. Adapted from [30]. The line represents the tradeoff between permeability and selectivity in current polymers.....	11
Figure 2–2. Phase diagram showing a casting solution inside the one phase region but close to the boundary between the one and two phase region. After the cast solution is placed in a nonsolvent coagulation bath, the nascent membrane moves into a region where the cast solution has two distinct phases.....	12
Figure 3–1. Chemical structures of (a) PBI and (b) Matrimid 5218.....	16
Figure 3–2. Films and membranes were optical clear. Stamp sizes (a)-(c) and (f) are 13.8cm ² . Stamp sizes for (d) and (e) are approximately 4cm ² . (a) Matrimid film (b) PBI/Matrimid film 25:75 (c) PBI/Matrimid film 50:50 (d) PBI/Matrimid film 75/25 (e) PBI film (f) PBI/Matrimid asymmetric membrane 50:50	22
Figure 3–3. PLM images of dense films and asymmetric membranes show no phase separation (a) Matrimid film (b) PBI/Matrimid film 25:75 (c) PBI/Matrimid film 50:50 (d) PBI/Matrimid film 75/25 (e) PBI film (f) PBI/Matrimid asymmetric membrane 50:50.....	22
Figure 3–4. Films were determined to be defect-free because permeability did not change with pressure.	24
Figure 3–5. XRD patterns for pure and blended dense films. 100 Matrimid and 25/75 PBI/Matrimid films were nearly indistinguishable as were 100 PBI and 75/25 PBI/Matrimid films. 50/50 PBI/Matrimid films were in between. (a) 100 PBI (b) 25/75 PBI/Matrimid (c) 50/50 PBI/Matrimid (d) 75/25 PBI/Matrimid (e) 100 PBI	26

Figure 3–6. (a) Mass remaining of pure and blended dense films with heating in N ₂ . (b) Mass remaining of pure and blended films with heating in air. All films performed similarly until 300°C.	26
Figure 3–7. Cloud point diagrams of 50/50 blends of PBI and Matrimid (open points). Pure Matrimid (closed points) are to the right of blends meaning less nonsolvent is necessary for blends to go from a homogeneous solution to an inhomogeneous solution[39].....	29
Figure 3–8. Colder coagulation baths result in lower permeances. The line represents the selectivity predicted by Graham’s law for transport governed by Knudsen diffusion. Over the range tested, coagulation bath temperature appears to have no effect on selectivity. All membranes underwent a 5 second forced evaporation period before being quenched in the coagulation bath.	31
Figure 3–9. Evaporation time affects H ₂ permeance and α_{H_2/N_2} . A defect-free, dense skin layer forms when the cast solution undergoes forced evaporation for a longer time before the nascent membrane is quenched in a coagulation bath. The coagulation bath was 12°C. The line for dense film was determined experimentally at 25°C and 10.2 atm.	32
Figure 3–10. a) Cross-section of a 50/50 PBI-Matrimid blend membrane with a H ₂ permeance of 80 GPU and $\alpha_{H_2/N_2} = 80$. The photomicrograph shows no macrovoids. b) A selective skin layer on a porous substructure.	33
Figure 3–11. XRD spectra for a Matrimid film, a PBI film and a 50/50 PBI-Matrimid asymmetric membrane. All are amorphous in structure. The 50/50 blend spectra is similar to the 100 Matrimid film.	34
Figure 3–12. Blended membranes demonstrate greater resistance to chemical attack by selected oxygenated aromatics at 50°C for 18 hours.	35
Figure 4–1. Ideal selectivities for several industrially important separations of blended dense PBI/Matrimid films a) 25/75 b) 50/50. Line added to guide the eye.	39
Figure 4–2. PBI/Matrimid blended dense films have linear relationships between ln(Permeability) and 1/T (1/K) from 21 to 200°C (a) 25/75 PBI/Matrimid film (b) 50/50 PBI/Matrimid film	41
Figure 4–3. The slow gases, CH ₄ and N ₂ , have larger permeances with increasing temperature while the fast gases, H ₂ and CO ₂ , show a maximum permeance at 50°C in 50/50 PBI/Matrimid asymmetric membranes. Line added to guide the eye.	42

Figure 4–4. Pure gas selectivities of a 50/50 PBI/Matrimid membrane for several commercially important processes are shown. Line added to guide the eye.	42
Figure 4–5. The thermal stability of asymmetric membranes was determined by cycling the membrane from room temperature to 200°C. Each time the temperature changed, permeance was measured.	43
Figure 4–6(a-d). Permeance falls from cycle one to cycle two but not between cycle two and three suggesting that the membrane is stable after the first annealing cycle.	44
Figure 4–7. Selectivity changes little between cycles. Line added to guide the eye.	45
Figure 4–8. N ₂ flux and selectivity are constant between 10 and 45 days at 200°C in an air environment.	45
Figure 4–9. The resistance to transport due to the substructure of an unannealed and an annealed membrane was investigated by removing membrane material with a sheet of fine grain sandpaper. The unannealed (virgin) membrane had selectivities below Knudsen diffusion after one sanding suggesting the substructure has little resistance to transport. The annealed membranes had Knudsen diffusion selectivity after 15 sandings, suggesting the substructure has significant resistance. (*After the fourth sanding of the virgin membrane, the gas flux exceeded the capacity of the test system.)	46
Figure 4–10. To test the stability of 50/50 PBI/Matrimid membranes at 300°C, the same temperature ramp experiment found in Figure 4–5 was performed, this time to 300°C. Membranes were held at 300°C for 18 hours in between cycles. (a) At all temperatures, H ₂ permeances were smaller after annealing at 300°C. (b) α_{H_2/N_2} at 200 and 300°C are higher after annealing at 300°C for 18 hours. After a second heating and annealing cycle, selectivities change little. Lines added to guide the eye.	47
Figure 4–11. Thermal annealing of membrane changes the distribution of spacing between polymer chains.	48
Figure 4–12. The mass remaining after heating in air shows annealing results in a slight increase in thermal stability.	49
Figure 5–1. Chemical structure of a) PBI and b) Matrimid 5218.	52
Figure 5–2. Matrimid and PBI points were calculated from group contribution while ethanol, 2-butanone, pentane and NMP were from tabulated data[56]. NMP is a known solvent for both Matrimid and PBI and is on the graph for reference. In general, ethanol should act	

more like a swelling agent for Matrimid while pentane will not. In general 2-butanone should act most like a swelling agent for PBI while ethanol and pentane are unlikely to have much effect..... 55

Figure 5–3. After one vapor treatment, almost all membranes treated with pentane were more selective. For those membranes treated with 2-butanone and ethanol, some membranes were more selective while others were not. Measurement error is the size of the points. (a) Selectivities of control membranes did not change (b) Pentane treatment (c) 2-butanone treatment (d) Ethanol treatment 56

Figure 5–4. Consecutive vapor treatments result in most membranes having lower permeances and selectivities. Control group remains unchanged. Measurement error is the size of the points. (a) Control (b) Pentane (c) 2-butanone (d) Ethanol 58

Figure 5–5. Vapor post treatments (a) after one treatment (b) after three treatments. Error bars represent the standard error of the mean change in selectivity. 59

Figure 5–6. After one liquid treatment, only a few membranes in the pentane group improved while almost all membranes in the 2-butanone group improved. Control group is the same as Figure 5–3a. Measurement error is the size of the points. (a) Pentane (b) 2-butanone 60

Figure 5–7. Consecutive liquid treatments result most membranes having lower permeances and selectivities. Control group is the same as Figure 5–4a. Measurement error is the size of the points. (a) Pentane (b) 2-butanone 61

Figure 5–8. Liquid post treatments (a) after one treatment (b) after three treatments. Error bars represent the standard error of the mean change in selectivity. 62

Figure A–1. Tan delta curves show that 25wt% and 50wt% PBI in Matrimid form immiscible blends 72

List of Tables

Table 2–1. Three different types of transport that can occur in a membrane. The type of transport depends on the pore size.	7
Table 3–1. Single gas permeability measurements for pure Matrimid and pure PBI films.....	17
Table 3–2. Location of $\tan \delta$ peaks. One peak means the sample is homogeneous. Multiple peaks mean the sample is heterogeneous.	24
Table 3–3. Single gas permeabilities and selectivities for blended dense films for permanent gases (measured at 10.2 atm, 22°C).....	24
Table 3–4. Density and fractional free volume of dense PBI/Matrimid films.....	25
Table 3–5. Films lost more mass in oxygenated environments than in N_2	27
Table 3–6. Properties of selected solvents and nonsolvents.....	28
Table 3–7. Hansen solubility parameters from [56]. Group contribution was used to calculate parameters for PBI and Matrimid. The difference in Hansen solubility parameters ($\Delta\delta$) as predicted by equation (20).	29
Table 3–8. Single gas permeance data for several sample blend membranes. Membranes underwent a 15 second evaporation time before immersion in a coagulation bath at 12°C. Measurements were taken at 25°C.....	34
Table 3–9. The average spacing between polymer molecules and densities for pure films and blended membranes	34
Table 4–1. Properties of a PBI and Matrimid 5218.....	38
Table 4–2. Activation energy for permeation for gases in blended PBI/Matrimid films	41
Table 4–3. Properties of blended membrane samples before and after heat treatment	49
Table 4–4. 50/50 PBI/Matrimid membranes are more stable with respect of temperature than pure Matrimid.	49
Table 5–1. Calculated Hansen solubility parameters for polymers, NMP and chosen treatments.	55
Table 5–2. Vapor pressures of chosen post-treatments	60

Acknowledgements

First, I must thank my advisor, Dr. Mary Rezac, for her support, and an infinite number of helpful discussions and suggestions. After being her student, I am a better at writing, presenting, experimenting, analyzing data, and drawing conclusions. She is everything a graduate student could ask for in an advisor and more.

Thank you to all my committee members. Dr. Peter Pfromm, your criticism has been invaluable but I am keeping the blue line. Thank you to Dr. Praveen Vadlani, Dr. Scott Staggenborg and Dr. Christine Aikens for serving on my committee and for their contributions to the thesis.

Thank you to all the Rezac and Pfromm group members for their help. I especially want to thank Liz Boyer, Ronald Michalsky, Fan Zhang, Michael Wales, John Stanford, Matthew Young, and Michael Heidlage for their friendship.

Lastly, I would like to thank my undergraduate workers Megan Smithmyer, Alexander Clark, Kabila Gana, and Victor Hugo Nassau Batista.

This material is based upon work supported by National Science Foundation Grant: From Crops to Commuting: Integrating the Social, Technological, and Agricultural Aspects of Renewable and Sustainable Biorefining (I-STAR); NSF Award No.: DGE-0903701 and the National Institute of Food and Agriculture, U.S. Department of Agriculture, under Agreement No. 2011-67009-20055.

Dedication

To all of the women who have encouraged me over the years especially my sister, Lynne; my mom, Patty; my aunt, Renee; my grandmother, Ronnie; and my great-grandmother, GB

Chapter 1 - Introduction

Separations processes account for about 45% of in-plant energy use in the petroleum and chemical industry. Distillation, drying and evaporation processes, all of which use thermal energy to induce a phase change in one or more components of a mixture in order to perform the separation, account for about 80% of this energy use[1]. Another way to separate mixtures is to use membranes. Membranes are attractive for separations because they have a small footprint, are modular in nature and, unlike other energy intensive separation processes; do not require a phase change for separation[2]. Membranes are currently used in a variety of industries including the medical industry to separate toxins in blood in dialysis patients, separating hydrogen from refinery streams for reuse and water from salt in desalination processes[3].

Membranes act as a barrier between two phases. By controlling the rate of passage of

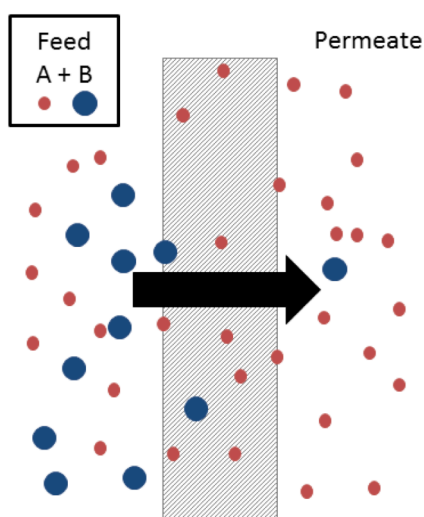


Figure 1–1. A membrane controls the transport of molecules through it. The feed consists of two components A and B. Because component B passes through the membrane more readily, the permeate will be enriched in component B.

species, membranes can produce streams enriched in one or more components. In Figure 1–1, the feed has two different molecules, A and B. Molecule B passes through the membrane more readily than A, so the permeate is enriched in B. What remains on the feed side, called the retentate, is enriched in A. Membranes control the rate of passage based on molecule size and shape, chemical nature or charge.

Membranes can be made of many different materials, including metals, ceramics and polymers. Graham noted in 1866 that palladium allowed the passage of H_2 but no other gases[4]. Ceramics are some of the most thermally and chemically stable materials known and are used in the industry where aggressive cleaning or sterilization is required[3]. Polymeric membranes are used because

they are inexpensive and easy to fabricate into a variety of configurations. Polymeric membranes are used in gas separation and reverse osmosis, and in micro and ultrafiltration applications[5].

The first membranes explored in a laboratory were made of pig bladders. Abbé Nolet, in 1748, used the word “osmosis” to describe water permeating through them. In 1831, Mitchell covered wide-mouth jars filled with different gases with a variety of materials including snapping turtle lungs and natural rubber, and observed that the balloons blew up with different velocities[6,7]. During the same period, Fick studied gas transport across nitrocellulose membranes and developed Fick’s first law describing how a substance will diffuse from a region of high concentration to a region of low concentration[8]. Graham made many important discoveries to membrane science, including but not limited to, quantitatively measuring gas permeation rates, proposing the solution-diffusion model for transport across a dense membrane, producing the first gas separation with a membrane, and noting that permeation rates through a membrane were dependent on temperature[9].

Membranes remained in the lab until the end of WWII, when membranes were used in Europe to test drinking water for pathogens. In the US, ceramic membranes were used to separate U^{235} from U^{238} for the manufacture of the atom bomb[3]. This separation was performed using Knudsen diffusion, which employed membranes with pore sizes approximately equal to the mean free path of the molecule. The separation factor for these membranes, as defined by Graham’s Law, was 1.004 for U^{235} over U^{238} , so many membranes were needed to achieve a pure product. This application was only possible because economics were not a consideration.

Membranes are defined by the amount of material that passes through them, their permeance, and their selectivity, α , towards one or more products. An ideal membrane allows a large amount of the desired components through, while being more impenetrable towards others. Using membranes at an industrial scale often requires large permeances and selectivities. Large permeances require thin separating layers but large selectivities require defect-free manufacturing. Manufacturing thin layers that are defect-free was not possible until the development of a perfected “phase inversion” process by Loeb and Sourirajan[10]. These membranes had a thin, defect-free skin layer supported by a porous support (Figure 1–2). These Loeb-Sourirajan membranes were first used to separate water from salt in reverse osmosis plants.

Attempts were made to use these membranes for gas separations, but because the effective sizes of gases are so much smaller than the effective size of water molecules, even a small defect is ruinous to the selectivity of a membrane. Henis and Tripodi at Monsanto solved this problem by coating the selective skin of a polysulfone membrane with a layer of highly permeable, but not particularly selective, polydimethylsiloxane (PDMS)[11,12]. The PDMS layer seals any defects in the selective skin layer of the polysulfone membrane. This dramatically increases the resistance to flow in the defects. This increase in resistance lowers the amount of

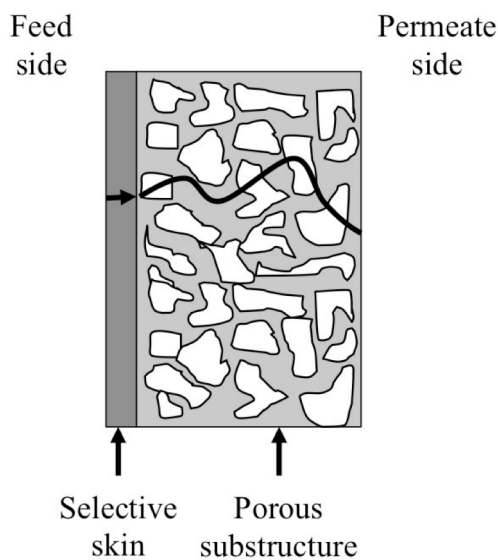


Figure 1–2. A model Loeb-Sourirajan membrane with a thin, dense selective skin layer which controls the separation. In this region, the gas meets most of the resistance to mass transfer. The bulk of the membrane thickness is a porous substructure that serves as a support for the skin layer. In this region, the gas meets little to no resistance.

include the recovery of extraction solvents in the vegetable oil industry, separations, concentrations and purifications in the pharmaceutical industry and separation and reuse of

gas passing through the defects. The resulting selectivity of the coated membrane is much higher than the uncoated membrane even though PDMS is much less selective than polysulfone. The first application of this type of membrane was to recover H_2 from purge gas streams in ammonia production facilities. This resulted in a significant energy savings. H_2 recovery operations have since expanded to refinery operations. Other gas separations include the production of N_2 from air and the removal of CO_2 from natural gas in order to meet pipeline specifications.

The first large-scale commercial liquid separation was reverse osmosis but membranes can perform other liquid separations. Organic solvent nanofiltration is attractive for the separation of organic compounds from aqueous and nonaqueous solutions. Separations that are of interest

homogeneous catalysts[13]. There is considerable interest in developing a polymeric nanofiltration membrane that can separate hot (up to 150°C) liquid feeds[14–17].

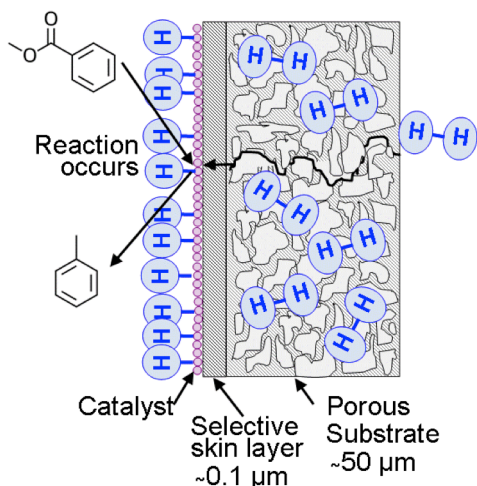


Figure 1–3. Schematic of a membrane reactor as a phase contactor

The liquid reagent is fed across the other side of the membrane. This setup differs from more traditional batch and slurry bed reactors because it avoids having the gaseous reagent first dissolve in the liquid reagent, and then diffuse to catalyst site. By precision delivering the gaseous reagent to the catalyst surface, lower pressures can be utilized, unwanted side products can be avoided and higher reaction rates can be realized[18].

In equilibrium reactions, there is both a forward and backwards reaction.



When the rate of forward reaction is the same as the backwards reaction, there is no further increase in the amount of either *C* or *D* formed. By using a membrane to selectively remove one of the products, the reaction is driven forward and higher conversion can be achieved.

Equilibrium reactions that have been studied with selective removal of a byproduct with a membrane include the removal of water in esterification and transesterification reactions and H_2 in dehydrogenation reactions[20,21].

Membrane reactors compete with trickle, packed, and slurry bed reactors. These types of reactors are not limited in their use by the thermal and chemical nature of the reagents. In polymeric membranes reactors, the polymer is a limiting factor. There are very few polymers

Another application of membranes is membrane reactors. There are a variety of ways to use a membrane as a reactor. Some of the most common setups use membranes as phase contactors in three-phase (gas-liquid-solid) reactions or to selectively remove a product to shift an equilibrium reaction forward[18–20]. When membranes are used in the phase contactor setup, catalyst is deposited on the surface of the membrane and the gaseous reagent is fed from one side where it diffuses through the membrane to the catalyst surface (Figure 1–3). The liquid

that can retain their properties at temperatures in excess of 100°C. Furthermore polymers can swell or dissolve in a variety of compounds, rendering them unusable.

Expanding the use of membranes in high temperature gas and nanofiltration separations, and in reactions, could benefit from the development of inexpensive polymeric materials that have more resistance to harsh thermal and chemical environments. Two options for developing polymers with better thermal and chemical resistance include designing new polymers or blending existing polymers. The development of new materials is a time-consuming and expensive process. Blending polymers can combine the advantages of several materials, without the drawbacks of developing new materials.

In 1846, Alexander Parkes noticed mechanical properties could be modulated by blending rubbery gutta-percha and glassy nitrocellulose[22]. This allowed these materials to be used in a wide range of consumer applications from buttons to furniture. As the number of known polymers has increased so has the number of patented blends[23–26]. Other benefits of blending polymers include modulating thermal and chemical resistance, biodegradability, cost and ease of processing.

In this dissertation, blends of polymers are explored to improve the thermal and chemical stability of gas separation membranes. In high temperature gas separations, such as H₂ and CO₂ in gasification operations, being able to separate gases without the need for cooling the feed would reduce the amount of energy and equipment required. These membranes will have characteristics appropriate for use in membrane reactor and nanofiltration applications as well.

Chapter 2 provides the background and theory related to membranes including transport across membranes, the phase inversion process for fabricating membranes, and behavior of polymer blends

Chapter 3 investigates properties of blended polybenzimidazole (PBI) and Matrimid 5218 dense films and asymmetric membranes. Dense films are useful for determining the intrinsic properties of the polymer including selectivity, permeability, and other properties. The fabrication of asymmetric membranes from PBI and Matrimid via phase inversion is discussed including the effects of casting conditions on final gas transport properties. A screening of the chemical resistance of these materials is investigated.

Chapter 4 investigates the properties of the dense films and the performance of asymmetric membranes fabricated in chapter 3 at temperatures above ambient conditions. The effect of thermal annealing on the gas transport properties of asymmetric membranes is probed.

Chapter 5 focuses on chemical post-treatments of membranes formed in chapter 3. The selectivity of a membrane with a defect-free skin layer should be the same as a dense film of the same material. If the selectivity is less than that of a dense film, it is assumed that the skin layer has defects. The skin layer of blended membranes is treated with benign liquid or vapor treatments to eliminate these defects.

Chapter 6 sums up major conclusions from each chapter and offers suggestions for future studies.

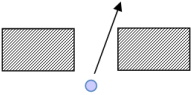
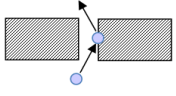
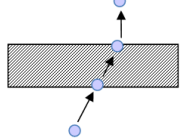
Chapter 2 - Background and theory

This research focuses on blended gas separation membranes with a dense selective skin layer on a porous substructure made by phase inversion. This chapter reviews fundamentals in transport theory of gases in porous and non-porous, or dense, materials, followed by an overview of the phase inversion process for producing integrally skinned asymmetric membranes. Lastly, properties of polymer blends are discussed.

1. Transport theory

Membranes separate components by controlling the rate of transport of these components through the membrane. There are several ways in which a molecule can be transported. The three different types of transport that are important to this work are: pressure-driven convective flow or Poiseuille flow, Knudsen diffusion, and solution-diffusion (Table 2–1). The size of the pores and the number of these pores in a membrane determines what molecules can be separated.

Table 2–1. Three different types of transport that can occur in a membrane. The type of transport depends on the pore size.

Pore size	Schematic	Type of transport
>1000Å		Poiseuille
500-1000Å		Knudsen diffusion
<5-10Å (dense)		Solution-diffusion

For permanent gases such as H₂, O₂ and N₂, Poiseuille flow will occur when pores in the membrane are greater than about 1000Å. Darcy's Law describes transport in a membrane with pores of this size:

$$J_i = K' c_i \frac{dp}{dx} \quad (2)$$

where J is the flux of component i , K' is a coefficient representing the membrane material. c is the concentration of the species of interest, p is pressure and x distance. The selectivity of a

membrane of this type for permanent gas separations would be 1, meaning no separation will occur.

Knudsen diffusion occurs when the pore size is about the same size as the mean free path of the molecule. The mean free path of a gas molecules, l , is calculated from the following equation:

$$l = \frac{k_B T}{\sqrt{2} \pi d^2 p} \quad (3)$$

where k_B is Boltzmann constant, T is the temperature, d is the diameter of the gas molecule, p is the pressure. The mean free path of a N_2 molecule at room temperature and a pressure of 50 psi is about 650 Å. As the pore size approaches the mean free path of the molecule, the penetrating molecule will interact with the walls more often. The molecule will be temporarily trapped when the molecule adsorbs on the walls of the pore. Larger molecules with larger mean free paths will interact more often with the pore walls than smaller molecules with smaller mean free paths. In this type of flow, Graham's law defines the selectivity of the membrane

$$\alpha_{A/B} = \sqrt{\frac{MW_B}{MW_A}} \quad (4)$$

where MW is the molecular weight of the smaller and larger molecule, A and B , respectively. For a purely Knudsen diffusion case, a material will have a separation factor of 3.74 for H_2 over N_2 .

The solution-diffusion model defines the transport of a penetrating molecule in a dense film and in the dense skin layer of the membrane[27]. Solution-diffusion occurs in three steps. First, the molecule absorbs into the skin layer. Then, the molecule diffuses through the membrane from a region of higher concentration to a region of lower concentration. Lastly, at the polymer-fluid interface, the molecule desorbs from the membrane. Different chemical species will have different rates of permeation because they have different rates of sorption and diffusion in the skin layer. Diffusion is a kinetic process determined by mass transfer while sorption is an equilibrium process determined by thermodynamics. The total transport is defined by the permeability coefficient

$$P = DS \quad (5)$$

where D is the diffusion coefficient and S is the sorption coefficient. Sorption is defined as

$$S = \frac{C}{p} \quad (6)$$

where C is the concentration of sorbed gas per unit volume of polymer and p is the pressure of the gas.

The ideal selectivity of a membrane for one gas over another is defined as the ratio of the pure gas permeabilities of the faster and slower gases, P_A and P_B , respectively.

$$\alpha_{A/B} = \frac{P_A}{P_B} \quad (7)$$

The selectivity of a membrane has a diffusive and a sorption selectivity

$$\alpha_{A/B} = \frac{D_A S_A}{D_B S_B} \quad (8)$$

Both components of selectivity are dependent on temperature[28]. Diffusive selectivity depends on the gas molecules having different mobilities in the polymer. The size and shape of the gas molecules, as well as the movement and packing of the polymer molecules determine this mobility. As temperature increases, the molecules have more thermal energy and the polymer chains move more freely. This movement limits the polymer's ability to distinguish gas molecules by their size and shape so diffusive selectivity falls. The sorption selectivity depends on the gas molecules having different condensabilities and interactions with the polymer. As temperature increases, the condensabilities of gases will fall. More readily condensable gases will act more like sparingly soluble gases. Sorptions of sparingly soluble gases, such as H_2 , are less affected by changes in temperature. Membranes that separate gases based on differences in equilibrium sorption at room temperature become less efficient as temperature increases.

The governing equation for transport is

$$J_i = -D_i \frac{c_{i0(m)} - c_{iL(m)}}{l} \quad (9)$$

where J is the flux of a chemical species i , D is the diffusion coefficient and l is the thickness of separating layer. The concentration of i in the skin layer of the membrane on the feed side is represented by the subscript $0(m)$ while the concentration of i in the skin layer of the membrane at the permeate interface is represented by the subscript $L(m)$.

Transport of gases through the selective skin layer occurs because there is a difference in chemical potential between the feed side and permeate side. This chemical potential difference can be due to a difference in gas composition, pressure, temperature, and electric potential[3]. If chemical potential is restricted to concentration and pressure, it can be written for a compressible gas as

$$\mu_i = \mu_i^o + RT \ln(\gamma_i n_i) + RT \ln \frac{p}{p_{i_{sat}}} \quad (10)$$

and for an incompressible fluid or for the membrane phase as

$$\mu_i = \mu_i^o + RT \ln(\gamma_i n_i) + v_i(p - p_{i_{sat}}) \quad (11)$$

where μ is the chemical potential of i , μ_i^o is a reference chemical potential, R is the gas constant, T is temperature, γ is the activity coefficient, n is the molar fraction, v is the molar volume, p is pressure and $p_{i_{sat}}$ is a reference pressure[29].

By equating chemical potentials in the bulk phase to chemical potentials of the gas in the membrane on both the feed and permeate side of the selective skin, the concentration of the gas in the membrane can be written in terms of the properties of the gas in the bulk on the feed side and permeate side.

$$c_{i_{0(m)}} = \frac{MW_i \rho_m \gamma_{i_0}^G}{\gamma_{i_{0(m)}} p_{i_{sat}}} p_{i_0} \quad (12)$$

$$c_{i_{l(m)}} = \frac{MW_i \rho_m \gamma_{i_l}^G}{\gamma_{i_{l(m)}} p_{i_{sat}}} p_{i_l} \quad (13)$$

where ρ is the molar density, and G is the activity coefficient of i in the gas phase. Substituting equations (12) and (13) into (9) we arrive at the equation

$$J = DS \frac{p_{i,0} - p_{i,l}}{l} \quad (14)$$

where S is the sorption coefficient defined as

$$S = \frac{m_i \rho_m \gamma_{i_0}^G}{\gamma_{i_{0(m)}} p_{i_{sat}}} \quad (15)$$

This equation tells us that the driving force for gas transport across a membrane is the difference between the partial pressure of the gas in the feed and the partial pressure of the gas in the permeate.

The ideal polymer for gas separations has large permeabilities and large selectivities. A larger permeability means for the same partial pressure of gas in the feed and permeate and the same skin layer thickness, the flux of gas will be larger. Large selectivities mean the permeate is more pure in the faster component. Polymers are measured against Robeson's "upper bound," a graph of permeability versus selectivity for selected gas pairs (Figure 2-1). Robeson has reported properties for several hundred polymers including all commercially relevant materials[30].

Polymers with large permeabilities typically have low selectivities while those with low permeabilities typically have high selectivities. The line is approximate and represents the upper limit of current materials. It has shifted up and to the right as new polymers are synthesized.

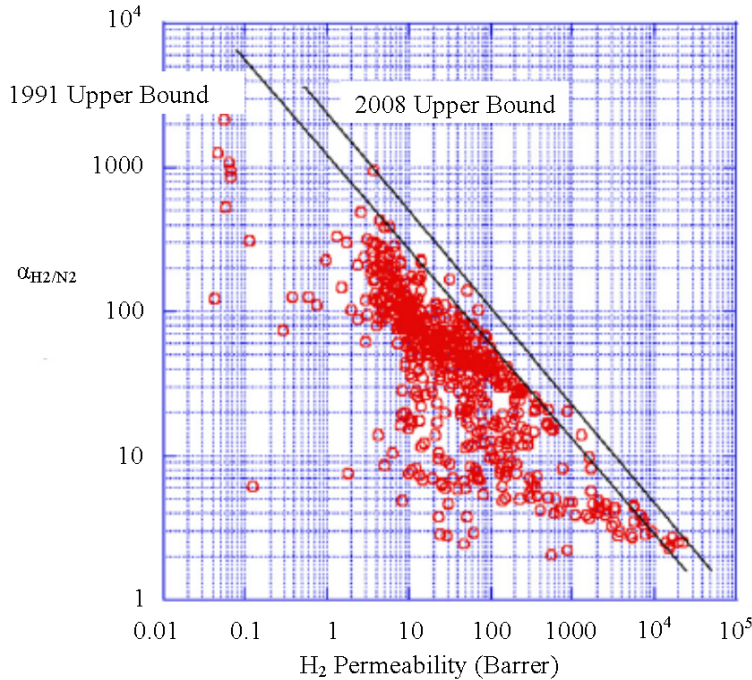


Figure 2–1. Adapted from [30]. The line represents the tradeoff between permeability and selectivity in current polymers.

2. Phase inversion

Asymmetric polymeric gas separation membranes can be fabricated as thin-film composites, where the selective skin layer and the porous substructure are fabricated separately, or by phase inversion, where the selective skin layer and the porous substructure are fabricated at the same time[10,31]. For phase inversion membranes, the polymer is dissolved in a mixture of solvents and a nonsolvent. The solution is stirred until it becomes homogenous. The addition of nonsolvent to the dope puts the solution close to the boundary where the solution would split into two phases (Figure 2–2). After an evaporation step, the nascent membrane is placed in a coagulation bath of nonsolvent, usually water, but sometimes an organic compound, such as methanol or acetone. The coagulation bath fluid can flow into the nascent membrane. This causes the cast solution to change from a state where it is most stable in a single phase to a state where it is most stable in two phases, a polymer-rich phase and a polymer-poor phase. When the solution moves from the one-phase region to the two-phase region above the critical point,

liquid-liquid demixing results in the nucleation and growth of the polymer-poor phase. The polymer-rich phase becomes the matrix of the membrane. The polymer-poor phase becomes the pores of the membrane. Liquid-liquid demixing will continue to occur until the glass transition (T_g) of the nascent membrane rises above the T_g of the surrounding system. At this point, further liquid-liquid demixing is not possible and the structure is “frozen” into place.

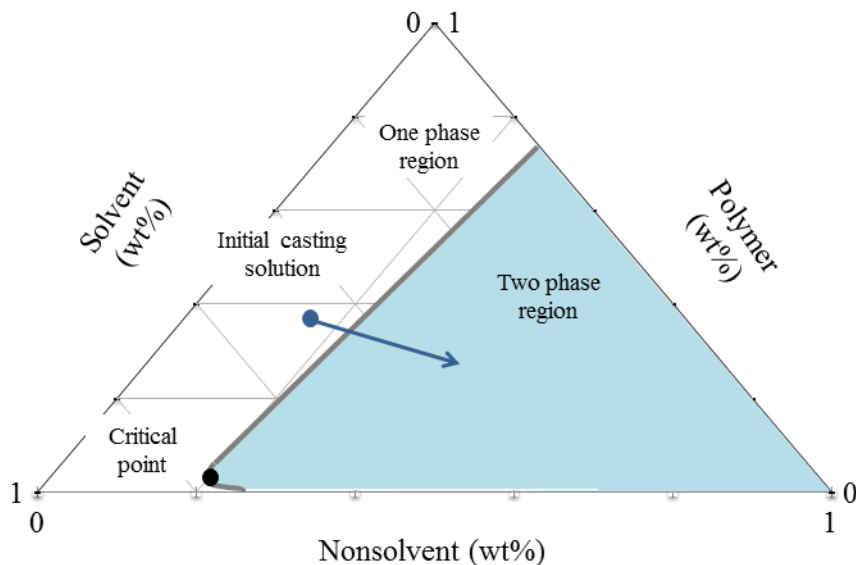


Figure 2–2. Phase diagram showing a casting solution inside the one phase region but close to the boundary between the one and two phase region. After the cast solution is placed in a nonsolvent coagulation bath, the nascent membrane moves into a region where the cast solution has two distinct phases.

3. Behavior of blends of polymers

Polymer blending allows the production of novel properties via the modification of existing materials without the need for the expensive and time-consuming process of developing new materials. While this work focuses on physically mixing different polymers, blends of polymers can also be fabricated chemically by copolymerizing different polymer repeat units. In both cases, a polymer blend can be miscible, i.e. blended on a molecular level, or immiscible, i.e. not blended on the molecular level. There are varying degrees of mixing that can occur in immiscible polymer blends. Immiscible blends consist of domains or phases of polymers with different compositions.

The miscibility of a blend can be determined by optical clarity and the presence of a single T_g . The T_g of a polymer is defined as the temperature where a polymer transitions from a

glassy to a rubbery state. In the glassy state, at temperatures below the T_g , the molecular movement of the polymer backbone is restricted. In the rubbery state, at temperatures above the T_g , coordinated movement of sections of the polymer backbone can occur. There are changes in several properties of the polymer at its T_g , including the specific volume, specific heat, and the storage modulus. The change in the storage modulus of the polymer occurs at the same time as a peak in the $\tan \delta$ curve, where δ is the ratio of the loss modulus to the storage modulus.

Because there are several measurable property changes at a polymer's T_g , there are several ways to measure the T_g and each will yield a slightly different number. For this work, $\tan \delta$ peaks were used to determine miscibility. With respect to $\tan \delta$ peaks, if two polymers are completely immiscible, a blend of the two will have two distinct $\tan \delta$ peaks at the same temperature as the pure components' T_g 's. If two polymers are miscible, a blend will have one narrow $\tan \delta$ peak at a temperature in between the pure components' T_g 's. If the polymers are neither completely immiscible or completely miscible, the peaks will be in between the pure components' T_g 's or can combine to form one broad $\tan \delta$ peak.

Many researchers have explored blends of polymers for membrane applications. There are a wide variety of polymers that are known to be miscible including a variety of polysulfones and polyimides, such as Ultrason and Matrimid; polyphenylsulfones and polyimides, such as Radel and Matrimid; copolyimides and polybenzimidazoles, such as P84 and PBI[23,32–34]. A variety of material properties, including mechanical and transport properties, change with the composition of the blend. Sometimes these properties change linearly with composition. In other cases, the properties differ either positively or negatively from simple linear relationships. For instance, Olabisi and Farnham found that the tensile strength of some miscible blends of poly(methyl methacrylate) and a polymer formed from α -methyl styrene, methyl methacrylate, and acrylonitrile were stronger than either of the homopolymers[35]. One important criterion in selecting a polymer for gas separation applications is the selectivity of the material towards one gas. In some cases, a miscible blend of polymers can show larger selectivities than either individual component[36].

Chapter 3 - Blended PBI/Matrimid films and asymmetric membranes; Fabrication and characterization

1. Introduction

Membranes can be more attractive than conventional separation techniques because they have a small footprint and do not require a phase change for separation to occur. Polymers are often used for gas separation membranes because they are inexpensive and easy to process into the desired morphology. Improvements to gas separation membranes that could be made include increasing the permeance and the separation factor and improving the thermal and chemical resistance to expand opportunities for using membranes to separate hot gas streams or those with aggressive contaminants. This paper focuses on improving the thermal and chemical resistance of polymeric membranes.

One strategy for improving the thermal and chemical resistance of polymeric membranes is to blend polymers. Polymer blending is attractive because it is reproducible and does not require the expensive development of new materials[33]. Polymer blending was first patented in the 1846 and it was noted that mechanical properties of materials could be modulated by blending two different polymers[37]. Polymer blending has been used to modulate mechanical properties, make it easier to process polymers, increase the thermal and chemical resistance of polymers and lower costs.

In general, polymers with large permeabilities and selectivities are attractive for use as a gas separation material. Other necessary characteristics include sufficient mechanical stability, resistance to plasticization, processibility, and low cost. When a single polymer does not meet all of these requirements, blending of two or more polymers can be useful[23,25,32].

A commercially available polybenzimidazole (PBI) and Matrimid 5218 (referred to as Matrimid after this) (Figure 3–1) were chosen as appropriate polymers for fabricating a thermally and chemically stable membrane. Matrimid has been studied extensively as a material for gas separation because of its attractive gas transport properties[38–41]. The published pure gas permeation data for Matrimid and PBI films is surprisingly varied. Table 3–1 provides H₂ and N₂ permeabilities and ideal H₂/N₂ selectivities. It is known that the measured permeabilities of these minimally sorbing gases are strongly dependent on temperature and nearly independent of

pressure. To allow for direct comparisons, the reported permeability values, P_T , were adjusted to 35°C using

$$P_{35^\circ\text{C}} = P_T \exp\left(\frac{\Delta E_p}{R}\left(\frac{1}{T} - \frac{1}{308}\right)\right) \quad (16)$$

using ΔE_p , the activation energy for permeation, values of 19.7 and 11.3 kJ/mol for N₂ and H₂, respectively[42]. Even after correcting for temperature, H₂ permeabilities range from 17.1 to 30.2 and H₂/N₂ selectivities range from 71 to 119 for Matrimid. For PBI, H₂ permeabilities range from 0.09 to 3.9 and H₂/N₂ selectivities range from 80 to 131. Matrimid has permeabilities at least an order of magnitude larger than PBI, making it the more attractive material from a gas transport perspective.

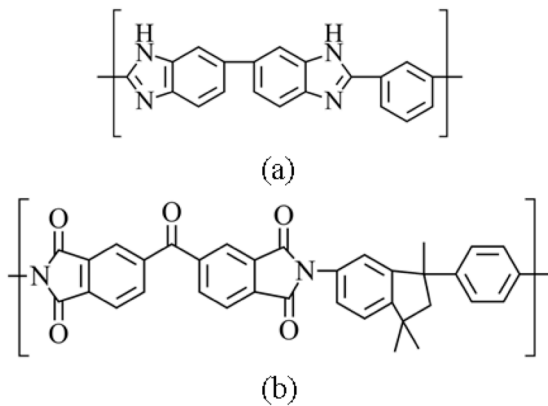


Figure 3–1. Chemical structures of (a) PBI and (b) Matrimid 5218

in general, PBI has more significant chemical resistance than Matrimid, dissolving in only a handful of highly polar, aprotic solvents[43]. Polyimides have attractive transport properties and are moderately attractive with respect to thermal and chemical stability, while PBI is extremely chemically and thermally stable. By blending Matrimid and PBI, the resultant properties should be intermediate between the two homopolymers.

Others have investigated dense films and asymmetric hollow fibers made of blends of these two polymers for liquid and gas separations. Dense films were miscible up to 20wt% PBI[44]. Asymmetric hollow fiber Matrimid/PBI membranes have been investigated for pervaporation applications including the separation of toluene/iso-octane and water/tert-butanol

The glass transition temperature (T_g) of a polymer is a very crude indicator of its potential operating temperature. While Matrimid has a high glass transition temperature of 323°C, PBI has an even higher T_g of 435°C. A higher T_g is associated with stiff polymer backbones. Stiffer backbones will have less mobility at higher temperatures. For a polymeric membrane to be able to distinguish gases at higher temperatures, a more rigid backbone is required. In

Table 3–1. Single gas permeability measurements for pure Matrimid and pure PBI films

Polymer	Testing T (°C)	Testing P (atm)	P _{N₂} (Barrer ^a)	P _{H₂} (Barrer ^a)	α _{H₂/N₂} [*]	P _{N₂} (Barrer ^a)	P _{H₂} (Barrer ^a)	α _{H₂/N₂} [*]
Matrimid			← At test temp →			← At T = 35°C →		
[84]	35	7.5	0.24	-	-	0.24	-	-
[85]	35	10	0.26	19.02	71	0.26	19.0	71
[86]	35	2.6	0.24	17.08	71	0.24	17.1	71
[87]	35	4	0.22	17.50	80	0.22	17.5	80
[88]	30	-	0.32	28.1	88	0.36	30.2	83
[33]	25	1	0.18	17.36	96	0.23	20.14	86
[89]	35	2.6	0.31	28.9	93	0.31	28.9	93
[39]	-	-	0.25	24	96	0.25	24	96
[47]	35	3.5	0.280	27.16	97	0.28	27.2	97
[42]	35	2	0.16	17.75	111	0.16	17.8	111
[40]	30	2	0.19	23.94	134	0.22	25.75	119
PBI								
[90]	25	-	-	0.09	-			
[91]	35	20.4	-	0.63	-			
[43]	30	-	0.049	3.9	80			
[92]	35	20	0.0048	0.6	131			

^a1 Barrer = 1×10^{-10} cm³(STP) cm/cm² s cmHg

systems using membranes with up to 20wt% PBI [44,45]. The authors found adding 3wt% PBI to Matrimid and annealing membranes at 250°C improved the selectivity of membrane in butanol/water separations. The increase in separation factor was attributed to the strong H-bonding between Matrimid and PBI, which inhibited swelling of the membrane by components in the feed[44,46]. Others have fabricated dense films with up to 75 wt% PBI for H₂ separations[47]. Increasing PBI content resulted in lower permeabilities and higher selectivities in H₂/N₂, H₂/CO₂ and CO₂/CH₄ separations. Dual layer hollow fibers with the outer fiber consisting of 50 wt% PBI in Matrimid on a polysulfone inner fiber have been investigated[48]. The selective layer, made of PBI and Matrimid, was not defect-free and a silicone rubber coating improved selectivities in H₂/CO₂ and CO₂/CH₄ separations by an order of magnitude.

The goal of this work is to determine if the thermal and chemical stability of Matrimid can be improved by the addition of PBI. This paper explores the production of flat sheet gas separation membranes with defect-free skin layers. By fabricating blend membranes without the need for a silicon rubber coating or a backing layer, we can probe the thermal and chemical resistance of the materials themselves.

The goal of this research is to extend the conditions where polymeric gas separation membranes can operate by fabricating and characterizing a more thermally stable membrane made from multiple polymers. Membranes that are thermally stable are also typically chemically resistant. By fabricating a thermally resistant membrane we will have likely fabricated one that can survive harsh chemical environments. By producing and characterizing these membranes, we hope to extend the range at which polymeric membranes can be used for gas separations facilitating the use of membranes into new applications.

2. Experimental

2.1. Materials

Reagent grade chemicals were purchased from Sigma-Aldrich and Cole Parmer. PBI (100 mesh powder) was obtained from PBI Performance Products (Charlotte, NC, USA). Matrimid was obtained from Archway Sales (Kansas City, MO, USA). Ultra high purity gases were obtained from Matheson TRIGAS and had a purity of at least 99.98%. All supplies were used as received.

2.2 Preparation of dense films

2.2.1 Preparation of Matrimid films

Solutions were prepared with Matrimid in dichloromethane (DCM). Films were made with 2 wt% polymer. After dissolution, the solution was poured into ring on a leveled glass plate. Solvent was allowed to evaporate for two days. Films were then washed with deionized (DI) water and placed in a vacuum oven at 200°C for 48 hours.

2.2.2 Preparation of blend and PBI films

All solutions were prepared with polymer in n-methylpyrrolidone (NMP). Films made with PBI/Matrimid mass ratios of 25/75, 50/50 were made with 20 wt% polymer, while 75/25 and pure PBI films were made with 2 wt%. For a 25/75 wt% PBI/Matrimid film, 2.5g of PBI was added to 40g of NMP. The solution was stirred at 120°C for 48 hours before lowering the solution temperature to 60°C. After holding at 60°C for 24 hours, 7.5g of Matrimid was added. The solution was stirred for two more days. The solution temperature was then lowered to 35°C and the stir bar stopped to allow for degassing. Films were cast 350µm thick on a glass plate and

placed in a vacuum oven equipped with a Edwards RV3 vacuum pump. Vacuum was established and the film was held at room temperature under vacuum for 24 hours. The oven temperature was raised to 100°C and held for 12 hours. Then the oven temperature was raised to 200°C and held for 24 hours. To remove the film from the glass plate, the plates were immersed in a bath of deionized (DI) water for 24 hours. After soaking in the water bath, films were swollen and slightly wrinkled. In order to remove the water while maintaining the integrity of the films, the films were solvent exchanged in three consecutive methanol baths followed by three consecutive hexane baths for 30 minutes each. Films were then placed in a hexane-enriched environment for 24 hours to slow the diffusion of hexane out of the film. Films were hung to dry overnight and were then placed in a vacuum oven at 200°C for 48 hours to remove residual solvent. Thermogravimetric analysis was used to check for the complete evaporation of solvent.

For 75/25 and PBI films, the solution was poured into rings on leveled glass plates. The glass plates were sitting on the surface of a mineral oil bath, such that oil was in contact with the bottom of the glass plate, but not the top surface, where the film was cast. The mineral oil, a heat transfer fluid, was held at 90°C and the plate was left on top of the bath for one day. Films were then processed identically to 25/75 and 50/50 blend films.

2.3 Cloud point measurements

PBI was added to solvent and stirred at 120°C for 24 hours. The temperature was lowered to 60°C and Matrimid was added and the solution stirred for a second day. All solutions, before adding nonsolvent, were about 10g total. The solution was checked to confirm that it was optically clear before nonsolvent was added drop-wise under N₂ until the solution became cloudy. Cloud point measurements were made at a solution temperature of 30°C.

2.4 Preparation of asymmetric membranes

Asymmetric membranes were prepared following the Loeb-Sourirajan phase inversion process[10].

2.4.1 Fabrication of Matrimid membranes

113g of NMP, 12g of tetrahydrofuran (THF), 30g of ethanol and 42g of Matrimid were stirred in a closed container at 60°C for 24 hours. The solution was allowed to cool to room temperature and the stir bar was stopped and the solution allowed to sit overnight in order to

degas the solution. Membranes were cast 350 μm thick and quenched in DI water. Membranes were solvent exchanged in 3 methanol baths followed by 3 hexane baths for 30 minutes each. Membranes were hung to dry and then placed in a vacuum oven at 110°C overnight.

2.4.2 Fabrication of PBI-Matrimid membranes

Membranes were made with a PBI/Matrimid mass percent of 50/50. 9.5g of PBI was added to a solution of 23g of NMP, 23g of dimethylformamide (DMF), and 9g of toluene and stirred for 24 hours at 120°C. The temperature was lowered to 60°C and 9.5g of Matrimid added. The solution was stirred for one more day. Then the solution temperature was lowered to 35°C and the stir bar stopped to allow for degassing. Membranes were cast 350 μm thick on a glass plate and underwent a period of forced evaporation before being quenched in a bath of DI water for 24 hours. The solution temperature at casting was 27°C. The membranes were solvent exchanged in three methanol followed by three hexane baths for 30 minutes each. Membranes were placed in a hexane-enriched environment for 24 hours to slow the diffusion of hexane out of the membranes and were then were hung to dry overnight. Following drying, membranes had a thickness of about 120 μm .

2.5 Characterization methods

2.5.1 Gas transport

Single gas permeabilities for dense films were measured using a constant volume-variable pressure system[49]. Measurements were taken at a feed pressure of 10.2 atm. The error due to the leak rate was less than 10% for the smallest permeability. Ideal gas selectivity was calculated as the ratio of single gas permeabilities:

$$\alpha_{A/B}^* = \frac{P_A}{P_B} \quad (17)$$

Single gas permeation of asymmetric membranes was measured using a constant pressure-variable volume system[50]. Measurements were performed with a differential pressure of 3.4 atm. In both the constant volume and constant pressure systems, the membrane area was 13.8 cm^2 and the temperature was between 20-25°C.

2.5.2 Density

Bulk densities of films and membranes were measured using a density gradient column composed of two solutions of aqueous calcium nitrate with different densities[51]. The 40 cm³ column had a linear increase in density from 1.20 to 1.50 g/cm³. The resulting uncertainty was 0.0075 g/cm³.

2.5.3 Miscibility

Visual inspection of the miscibility of polymers in films and asymmetric membranes was studied using a Nikon eclipse LV100 polarized light microscopy (PLM). Mechanical properties and T_g of films were determined using a Perkin-Elmer dynamic mechanical thermal analysis (DMTA). The glass transition temperature was determined as the peak of the tan δ curve. Samples were heated from 200 to 475°C at 10°C/min. Samples were analyzed in compression mode in an aluminum sample pan.

2.5.4 Morphology

The morphology of asymmetric membranes was investigated using a Hitachi S-3500N scanning electron microscope(SEM) with a Through Lens Detector at 5.0kV. Membranes were first fractured after dipping in liquid N₂ and then coated with a thin layer of gold and palladium.

2.5.5 Chain packing

A Rigaku Miniflex II (Japan) X-ray diffractometer (XRD) with Cu Kα radiation source was used to investigate the arrangement and chain spacing of polymer molecules. The dominant d-spacing between polymer chains was calculated using Bragg's law:

$$n\lambda = 2d\sin\theta \quad (18)$$

where n is an integer, λ is the wavelength of the x-ray (0.154 nm), d is the spacing between polymer chains and θ is the diffraction angle where the peak occurs.

2.5.6 Thermal and chemical stability

Decomposition with temperature was quantified using a Perkin Elmer Pyris 1 thermogravimetric analyzer (TGA) (Norwalk, CT). About 5 mg of sample was placed in a pan. Samples were heated from room temperature to 100°C at 25°C/min. Sample was held at 100°C

to desorb water and other residual sorbed species and then heated from 100 to 650°C at 10°C/min.

The procedure for quantifying the chemical resistance of membranes by determining the amount of mass that did not dissolve is published elsewhere[52]. Several oxygenated aromatics were selected to test the chemical resistance of homopolymers and blends because they are chemically similar to a variety of the solvents for both polymers. After soaking the membranes in a aromatic compound at 50°C for 16 hours, any macroscopic pieces of membrane remaining were removed and the solution filtered using a preweighed PTFE filter. To ensure complete filtration of the solution, 1 mL of NMP was used to remove any residual solution from the headspace of the filter. The NMP and chemical was removed from the filter and remaining membrane pieces by heating in a vacuum. The insoluble mass was calculated from the weighed residue of both the macroscopic membrane and the residue remaining in the filter.

3. Results and discussion

3.1. Appearance of dense films and asymmetric membranes

All films were optically clear (Figure 3–2). The intensity of color increased with PBI content and ranged from amber (pure Matrimid) to dark brown (PBI). The 50/50 PBI-Matrimid membranes were optically clear but were different on the skin and porous side. The skin layer was shiny while the porous side was more opaque. There was very little difference in the color between the 50/50 film and the 50/50 membrane. Polarized light microscopy images show no phase separation on the micron scale (Figure 3–3).

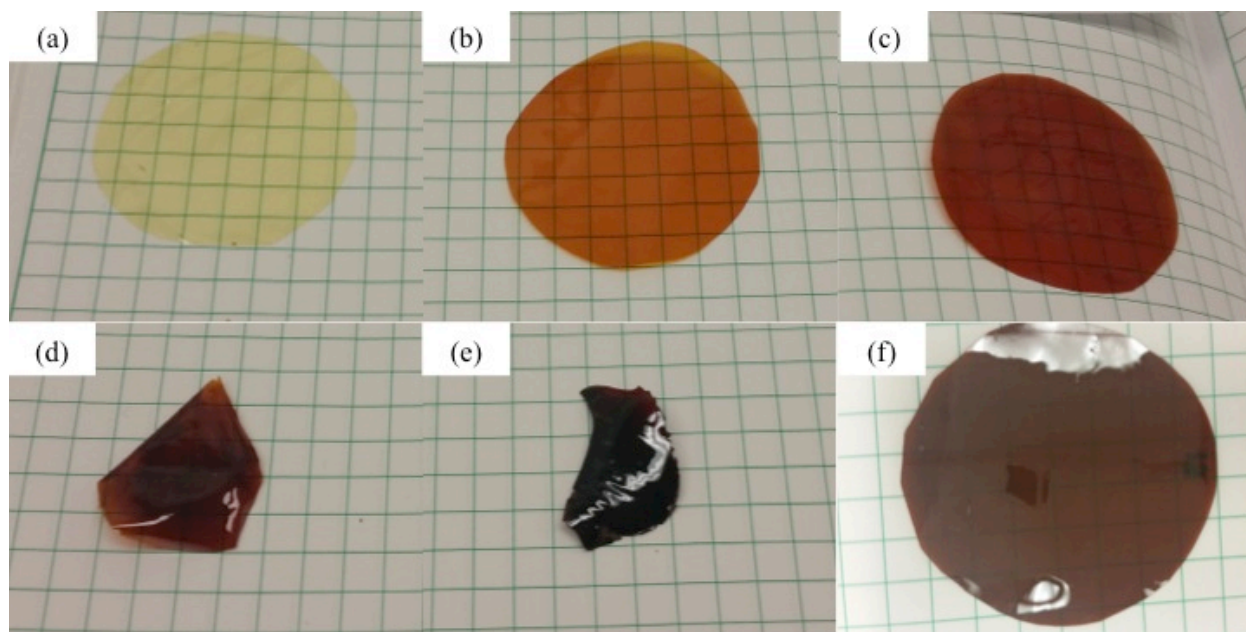


Figure 3–2. Films and membranes were optical clear. Stamp sizes (a)-(c) and (f) are 13.8cm². Stamp sizes for (d) and (e) are approximately 4cm². (a) Matrimid film (b) PBI/Matrimid film 25:75 (c) PBI/Matrimid film 50:50 (d) PBI/Matrimid film 75/25 (e) PBI film (f) PBI/Matrimid asymmetric membrane 50:50

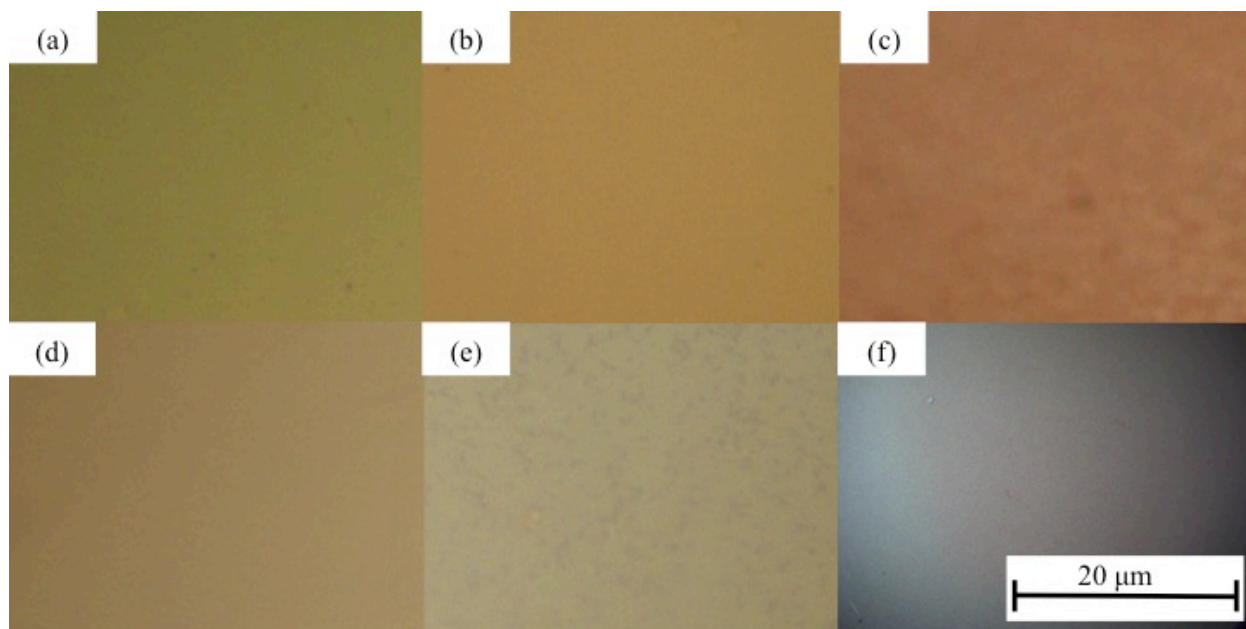


Figure 3–3. PLM images of dense films and asymmetric membranes show no phase separation (a) Matrimid film (b) PBI/Matrimid film 25:75 (c) PBI/Matrimid film 50:50 (d) PBI/Matrimid film 75/25 (e) PBI film (f) PBI/Matrimid asymmetric membrane 50:50

3.2. Miscibility of dense films

The location of the peak of the $\tan \delta$ curve can be found in Table 3–2. Pure Matrimid has a single $\tan \delta$ peak, indicating it is homogeneous. The blends listed have $\tan \delta$ peaks close to pure Matrimid and literature values of pure PBI peaks[44]. This indicates the blends are immiscible. The $\tan \delta$ curves can be found in the appendix.

Table 3–2. Location of $\tan \delta$ peaks. One peak means the sample is homogeneous. Multiple peaks mean the sample is heterogeneous.

Sample	Location of $\tan \delta$ peak(s) ($^{\circ}\text{C}$)
100 Matrimid	344
25/75 PBI/Matrimid	333, 400
50/50 PBI/Matrimid	359, 432

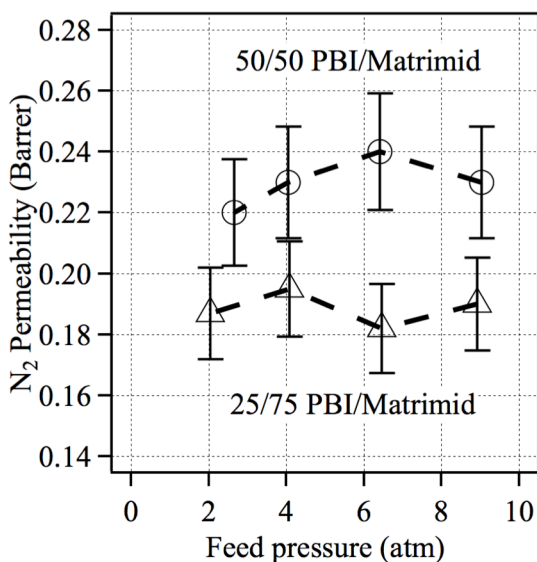


Figure 3–4. Films were determined to be defect-free because permeability did not change with pressure.

Blend permeabilities are intermediate between the homopolymers and roughly follow established blending rules.

3.3. Gas transport properties of dense films

To confirm that films were defect-free, N_2 permeability was measured at four different feed pressures between 2 and 9 atm at room temperature (Figure 3–4). Films that demonstrated consistent permeability, independent of pressure, were considered defect-free. All films were about 50 μm thick.

Measured room temperature permeabilities for five permanent gases and selectivities for several industrially important separations are reported in Table 3–3. For the 25/75 PBI-Matrimid film, permeabilities and selectivities are on the same order of magnitude as other literature values[47]. However, the calculated $\alpha_{\text{H}_2/\text{N}_2}$ was much lower, 84 versus 121 [47]. This range of values is comparable to the range of values found for the homopolymers (Table 3–1). These differences could be due to differences in the fabrication process, thermal histories or aging of the

Table 3–3. Single gas permeabilities and selectivities for blended dense films for permanent gases (measured at 10.2 atm, 22°C)

Film	Single gas permeability (Barrer ^a)					Ideal gas selectivity		
	P _{N2}	P _{CH4}	P _{O2}	P _{CO2}	P _{H2}	α _{H2/N2}	α _{CO2/CH4}	α _{O2/N2}
0/100 Matrimid ^b	0.22	0.16	-	4.9	14.0	62.5	31.8	-
25/75 PBI/Matrimid	0.19	0.14	1.3	5.2	16.0	84	37	7
50/50 PBI/Matrimid	0.18	0.12	1.2	4.7	15.6	89	38	7

^a1 Barrer = 1x10⁻¹⁰ cm³(STP) cm/cm² s cmHg ^bAt 35°C from [55]

Bulk properties of the dense films can be found in Table 3–4. Density increases with percent PBI. Group contribution data was used to calculate the van der Waals volume, V_w , and molecular weight, MW, of Matrimid and PBI[56]. Group contribution allows properties of polymers, which have a large variety of chemical backbones and side groups, to be calculated by splitting the large molecule into smaller groups. The properties of the smaller groups are found in tabulated data. The properties of the total polymer molecule can be calculated by a summation of the properties of the all of the smaller groups making up the polymer molecule. V_w and MW of the blends were calculated as means of the pure components. The fractional free volume, FFV , was calculated from the occupied volume, V_o , and the specific volume, V_s ,

$$FFV = 1 - \frac{V_o}{V_s} \quad (19)$$

Table 3–4. Density and fractional free volume of dense PBI/Matrimid films

Membrane	ρ (g/cm ³)	V_w (cm ³ /mol) ^a	MW (g/mol)	V_o (cm ³ /g)	V_{sp} (cm ³ /g)	FFV
Matrimid	1.254 ^b	288	553	0.677	0.797	0.151
25/75 PBI-Matrimid	1.269	256	492	0.677	0.788	0.141
50/50 PBI-Matrimid	1.293	224	431	0.676	0.773	0.125
75/25 PBI-Matrimid	1.315	192	369	0.676	0.760	0.111
PBI	1.320	160	308	0.675	0.757	0.109

^a[55] ^bCalculated from [56]

All values used to calculate FFV are within 13% of others[47]. Small differences in measured densities could be the result of differences in film processing while differences in calculated V_w could be the result of different group increments used. Even though there are small differences in calculated and measured values, all trends are similar. Most importantly, the FFV of blends decreases with percent PBI.

XRD patterns for pure and blended films can be found in Figure 3–5. All XRD spectra showed a “halo” which is characteristic of an amorphous structure. 100% Matrimid and 25/75 PBI/Matrimid blends are indistinguishable as are 100 PBI and 75/25 PBI/Matrimid. Films with more PBI have curves shifted to the right of the spectra, where d-spacings are smaller. This, coupled with the decreasing FFV with the addition of PBI, correlates with the drop in permeability with increasing amounts of PBI.

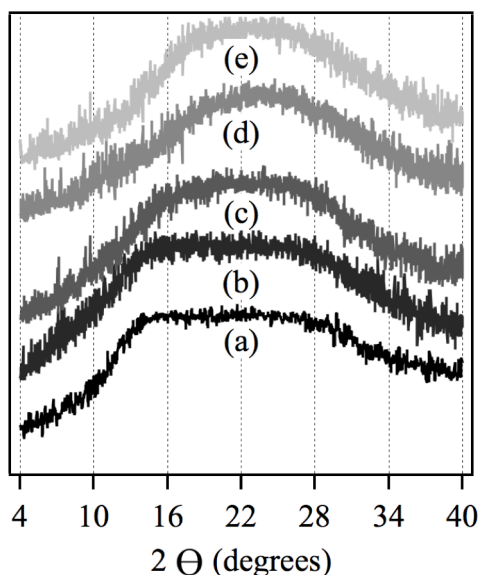


Figure 3–5. XRD patterns for pure and blended dense films. 100 Matrimid and 25/75 PBI/Matrimid films were nearly indistinguishable as were 100 PBI and 75/25 PBI/Matrimid films. 50/50 PBI/Matrimid films were in between. (a) 100 PBI (b) 25/75 PBI/Matrimid (c) 50/50 PBI/Matrimid (d) 75/25 PBI/Matrimid (e) 100 PBI

PBI. The 75/25 film lost slightly more mass than the pure PBI film between 100 and 200°C which is attributable to this water. All films lost more mass in air than in N₂. This could be due to desorbing water or solvent. Also, in the presence of O₂, polymers can undergo thermal oxidation[58]. Without O₂, the only way for polymer to lose mass is thermal degradation.

Thermal resistance was quantified by measuring the amount of mass remaining as the sample was heated. Figure 3–6 shows the thermal decomposition in N₂ and air of pure and blended films. Blended films retain mass better than 100% PBI at temperatures below 600°C in N₂ and 550°C in air. Table 3–5 compares the temperature at which 5 wt% loss of sample occurs in N₂ and air as well as the residual mass at 640°C for pure and blend films. Matrimid retained more mass than PBI from 350 until 600°C, while above 600°C PBI retained more mass than Matrimid. The blended films were in between the pure films with the exception of the 75/25 PBI/Matrimid film in N₂. In between 325 and 450°C, the blend film retained less mass than the 100 PBI film. It is known that PBI will retain water up to about 150°C so best attempts were made to store films in a vacuum oven until testing[57]. This was more successful for films with lower wt%

Given that PBI has a higher T_g than Matrimid, it was expected that PBI would retain more mass than Matrimid across the temperature range expected. The onset of decomposition for PBI, and blends, is 325 and 300°C in N_2 and air, respectively. Asymmetric gas separation membranes, with their thin (<1000 nm) skin layer, will be sensitive to even small amounts of mass loss. Even though PBI has a T_g of 435°C, it is unlikely that blend membranes will not continue to separate gases at temperatures in excess of 300°C.

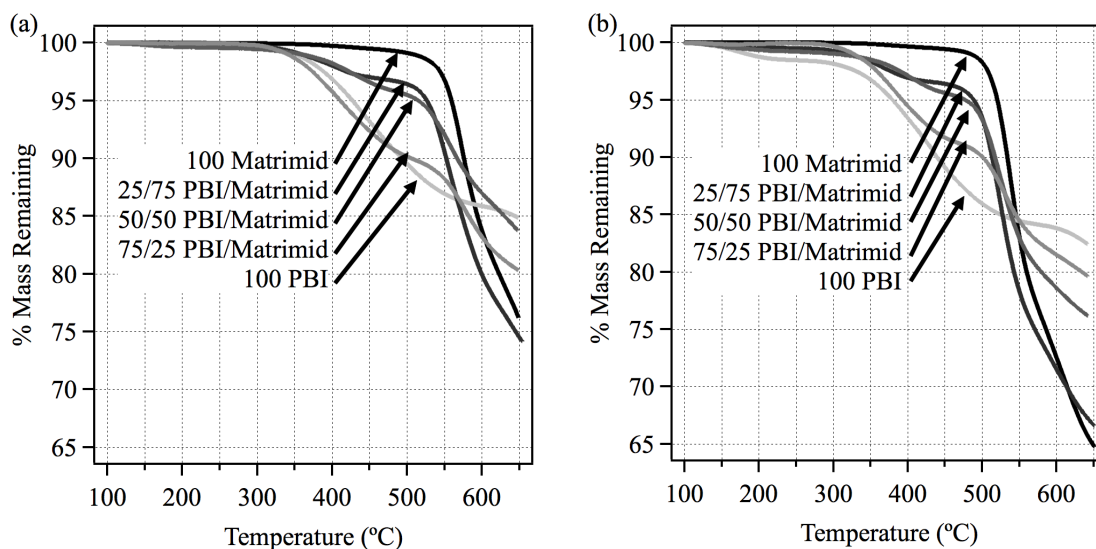


Figure 3–6. (a) Mass remaining of pure and blended dense films with heating in N_2 . (b) Mass remaining of pure and blended films with heating in air. All films performed similarly until 300°C.

Table 3–5. Films lost more mass in oxygenated environments than in N_2 .

Sample	Temperature at 5% weight loss		Residual mass at 640°C	
	N_2	Air	N_2	Air
100 Matrimid film	560	520	77	65
25/75 PBI/Matrimid film	525	490	75	67
50/50 PBI/Matrimid film	515	476	84	76
75/25 PBI/Matrimid film	410	392	81	79
100 PBI film	425	380	85	82

3.4. Cloud point diagrams

For an asymmetric membrane to be fabricated by phase inversion, the polymer must first be dissolved in solution. PBI is soluble in only a few compounds including NMP, DMF,

dimethylacetamide (DMAc), dimethyl sulfoxide (DMSO), and sulfuric acid. DMSO and sulfuric acid were not considered because they have insufficient volatility and human health concerns. It has been suggested that DMAc requires LiCl as a stabilizer for PBI to remain in solution[59]. Removing this salt after membrane preparation would have increased the complexity of the casting process, so NMP and DMF were the focus of our efforts. The number of nonsolvents that could be chosen is considerably larger. Acetone, ethanol, and toluene were investigated as possible nonsolvents. Table 3–6 shows the density and boiling point of the solvents and nonsolvents studied. Table 3–7 shows the solubility parameters for the solvent, nonsolvents, and polymers. The solubility parameters are broken down into their three components: dipole, polar and hydrogen bonding. The difference in Hansen solubility parameters can be calculated from

$$\Delta\delta = \left[(\delta_{d,P} - \delta_{d,S})^2 + (\delta_{p,P} - \delta_{p,S})^2 + (\delta_{h,P} - \delta_{h,S})^2 \right]^{1/2} \quad (20)$$

Table 3–6. Properties of selected solvents and nonsolvents

Chemical	ρ^a (g/cm ³)	Boiling point ^a (°C)
NMP	1.028	202
DMF	0.949	153
Toluene	0.867	111
Acetone	0.792	57
Ethanol	0.789	79

^a[56]

where δ is the solubility parameter from the literature for the solvents and nonsolvents and calculated from group contribution for the polymers[56]. The subscripts d , p , and h are the dipole, polar, and hydrogen bonding contributions, respectively, to the total solubility parameter. The subscripts P and S represent polymer and solvent. For the polymer to dissolve, the differences in solubility parameters must be small. The solvents NMP and DMF are

good solvents for Matrimid, with $\Delta\delta$ being 6.0 and 5.3 respectively. They are solvents for PBI, with, $\Delta\delta$ being 9.3 and 12.1; however DMF requires elevated temperatures to promote PBI dissolution.

Table 3–7. Hansen solubility parameters from [56]. Group contribution was used to calculate parameters for PBI and Matrimid. The difference in Hansen solubility parameters ($\Delta\delta$) as predicted by equation (20).

	Solubility parameter ^a ((MJ/m ³) ^{1/2})			$\Delta\delta$ (MJ/m ³) ^{1/2}	
	δ_d	δ_p	δ_h	PBI	Matrimid
N-methylpyrrolidone	17.9	12.3	7.2	9.3	6.0
Dimethylformamide	17.4	13.7	11.3	12.1	5.3
Toluene	18.0	1.4	2.0	10.5	12.0
Acetone	15.5	10.4	7.0	10.8	8.1
Ethanol	15.8	8.8	19.5	18.0	5.6
PBI	25.7	8.1	4.5	-	-
Matrimid	17.8	8.4	11.7	-	-

^aSubscripts represent the contributions of d = dispersion, p = polar, h = hydrogen bonding solubility parameters

Figure 3–7 shows cloud points for a solution of NMP with equal parts PBI and Matrimid and three nonsolvents. The area to the left of the points represents the one-phase region, while the area to the right of the points represents the two-phase region, where the solution splits into a polymer-rich phase and a polymer-poor phase. Knowing the cloud point location allows casting

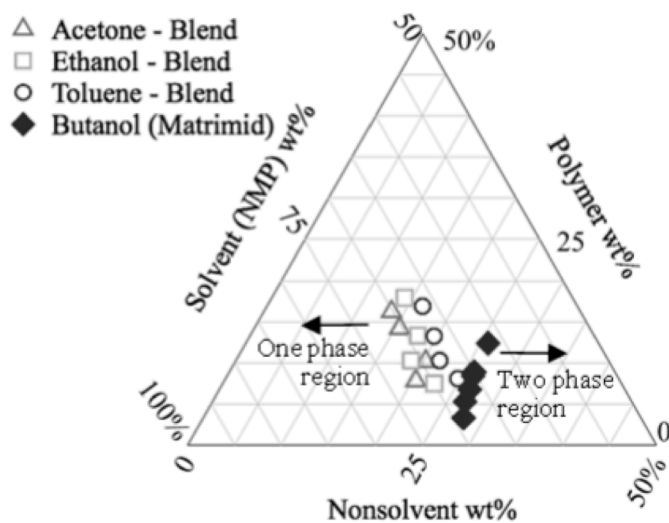


Figure 3–7. Cloud point diagrams of 50/50 blends of PBI and Matrimid (open points). Pure Matrimid (closed points) are to the right of blends meaning less nonsolvent is necessary for blends to go from a homogeneous solution to an inhomogeneous solution[39].

solutions to be intelligently designed because casting solutions must be homogenous, or in the one-phase region to the right of the cloud points, but close to the inhomogeneous region, or close to the cloud points[60].

All PBI and Matrimid blend cloud points are to the left of the pure Matrimid data[39]. In the blend case, smaller

amounts of nonsolvent are required for the solution to pass from the one-phase region to the two-phase region than in the pure Matrimid case. The blend solution requires less nonsolvent to pass from the one to two-phase region because PBI, which requires temperatures and pressures above ambient or a stabilizer to form a solution, is more difficult to dissolve.

Determining the exact location of the cloud point was difficult because the solution would clump before it would turn turbid. Best attempts were made to avoid clumping by adding solution drop-wise; however as the solution approached the cloud point a single drop could result in clumping. The dark color of the solution made clump detection difficult, especially as the volume of the solution increased with addition of nonsolvent. Clump detection was determined by tilting the jar back and forth and examining the portion of solution that stuck to the wall. This process was repeated several times. As a result, it is possible that the first clump was not detected. The detection of a clump was noted as a cloud point if the clump did not disappear after stirring for 4 hours. Acetone and ethanol reach the two phase region before toluene. According to the solubility parameters, toluene acts most like a solvent for PBI while ethanol acts most like a nonsolvent for PBI. The opposite is true for Matrimid. PBI is more difficult to go into solution, so it is possible that the boundary between the one and two-phase region is determined more by how strongly a nonsolvent acts as a nonsolvent for PBI than for Matrimid.

3.5. Optimizing membrane fabrication procedures for asymmetric membranes: Comments, and the importance of coagulation bath temperature and evaporation time on gas transport properties

Forming an asymmetric membrane from a 50/50 blend of PBI and Matrimid was the focus of these efforts because this blend had optimum film properties. With respect to thermal and chemical stability, higher wt% PBI is desirable because PBI has a higher T_g than Matrimid. The higher the T_g , the more rigid the polymer backbone is, and the more likely the polymer is to be able to retain its separating ability at temperatures above ambient, but below its T_g . From a chemical resistance perspective, PBI is considered to be more stable than Matrimid, as PBI dissolves in only five solvents, while Matrimid dissolves in 13.

Pure PBI, however, is difficult to dissolve and brittle when dry. A solution of 1wt% PBI in NMP will turn turbid, indicating an inhomogeneous solution, within a few weeks at room temperature, rendering it useless for casting. Larger wt% PBI solutions will turn turbid even faster and the situation becomes direr when nonsolvents are introduced to the casting solution. In terms of brittleness, there was little difference in handling of 25/75 and 50/50 PBI/Matrimid films; however 75/25 blends cracked easily. Furthermore, there was a large decrease in permeabilities between pure Matrimid and 25/75 films; 22.1 Barrer for H₂ permeability is the average of value of Table 1 versus 16.0 Barrer, but the drop in permeability between 25/75 and 50/50 blends was small, 16.0 versus 15.6 Barrer. 50/50 PBI/Matrimid asymmetric membranes

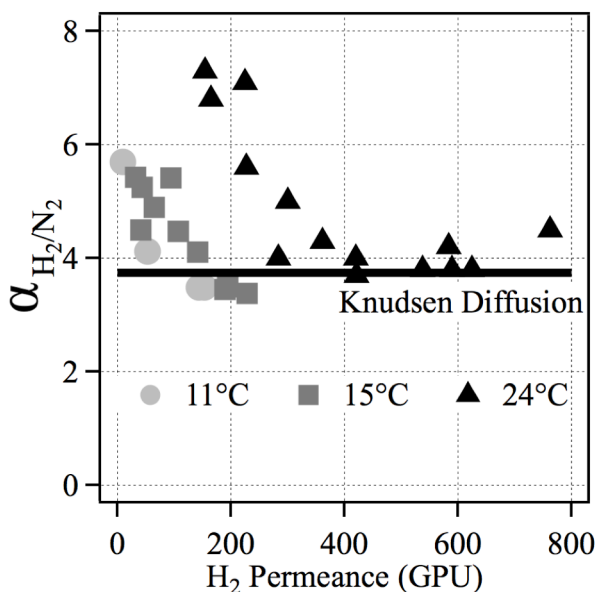


Figure 3–8. Colder coagulation baths result in lower permeances. The line represents the selectivity predicted by Graham’s law for transport governed by Knudsen diffusion. Over the range tested, coagulation bath temperature appears to have no effect on selectivity. All membranes underwent a 5 second forced evaporation period before being quenched in the coagulation bath.

were fabricated because 50wt% PBI was the maximum amount of PBI that resulted in a casting solution that remained homogenous at room temperature for useful time frames and resulted in membranes that were easily handled after fabrication.

A nonsolvent with high boiling point was desired because elevated temperatures were required for PBI to dissolve. Toluene was chosen as the nonsolvent for membrane fabrication because of its higher boiling point. Because toluene is only sparingly soluble in water, an excess of DI water was used in the coagulation bath (5L DI water/cast membrane sheet).

The effect of the temperature of the coagulation bath on gas transport properties is shown in Figure 3–8. In general, warmer bath temperatures

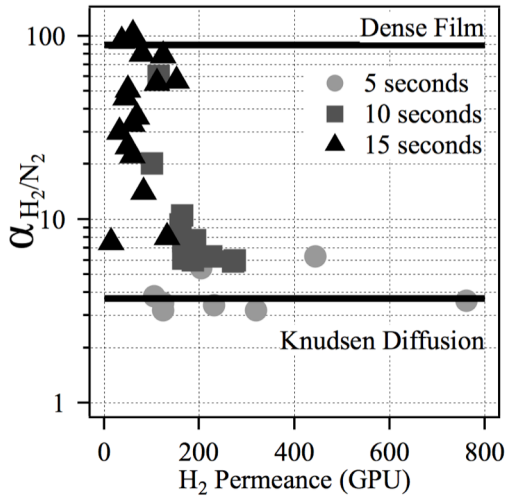


Figure 3–9. Evaporation time affects H₂ permeance and α_{H_2/N_2} . A defect-free, dense skin layer forms when the cast solution undergoes forced evaporation for a longer time before the nascent membrane is quenched in a coagulation bath. The coagulation bath was 12°C. The line for dense film was determined experimentally at 25°C and 10.2 atm.

resulted in higher permeances. All membranes had selectivities at or slightly above the range of Knudsen diffusion. This suggests a skin layer with defects on the order of magnitude of the mean free path of the N₂, 65 nm.

Evaporation time is measured as the time the nascent membrane was held in the hood after casting before being immersed in the quench bath. Small changes in evaporation time causes significant changes in the gas transport properties of the resultant membranes (Figure 3–9). Shorter evaporation times had large permeances but Knudsen diffusion selectivities. Longer evaporation times had lower permeances but selectivities near that of a defect-free dense film. Several membranes had selectivities above that measured by a dense film.

The effective skin layer thickness can be estimated from permeability and pressure-normalized flux data:

$$l = \frac{P_i}{J_i} (p_{i,0} - p_{i,l}) \quad (21)$$

where l is the effective skin layer thickness, P_i is the permeability of component i , J is the flux, and $p_{i,0}$ and $p_{i,l}$ are the partial pressures of gas on the feed and permeate sides, respectively. The estimated thickness of defect-free membranes that underwent a 15 second evaporation time is between 1,258 and 4,149 nm. This is much larger than expected as polymeric gas separation membranes with H₂ permeances around 100 GPU, have selective skin layers of less than 1000 nm. This estimation of the skin layer thickness could be larger than the true thickness of the skin layer because the skin layer is not uniform in thickness or there is resistance to transport in the substructure of the membranes.

The best membranes were then tested for single gas permeances in CH₄, O₂ and CO₂. Data for three such membranes can be found in Table 3–8.

3.6. Characterizing 50/50 asymmetric blend membranes

SEM confirms the formation of a skin layer on top of the porous substructure (Figure 3–10). The skin layer thickness measured from SEM images is approximately 600 nm. The substructure has

no macrovoids. Macrovoids are undesirable because macrovoids can collapse and compromise the integrity of the membrane during high-pressure operations. The membranes did not turn turbid with immersion. In fact, slight turbidity only appeared when membranes were removed from the last hexane solvent exchange bath and placed in the hexane-enriched environment. Turbidity is associated with phase separation. Fast precipitation rates can be associated with finger-like or macrovoids, while slower precipitation rates are associated with a sponge-like structure[61]. The slow turbidity change in these membranes and absence of macrovoids suggests a slow demixing process.

Chain packing of films and membranes was investigated with XRD. The Matrimid film has a larger average d-spacing, 4.3Å, than PBI film, 3.7Å (Table 3–9). 50/50 blend membranes have two distinct most common spacings at 3.5 and 5.2Å and a distribution of spacing most similar to Matrimid.

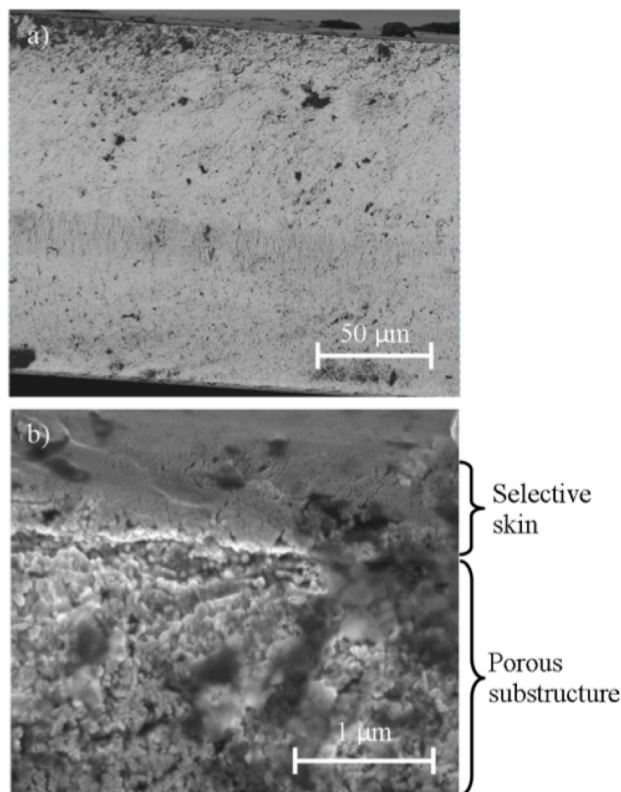


Figure 3–10. a) Cross-section of a 50/50 PBI-Matrimid blend membrane with a H₂ permeance of 80 GPU and $\alpha_{\text{H}_2/\text{N}_2} = 80$. The photomicrograph shows no macrovoids. b) A selective skin layer on a porous substructure.

Table 3–8. Single gas permeance data for several sample blend membranes. Membranes underwent a 15 second evaporation time before immersion in a coagulation bath at 12°C.

Membrane	Single gas permeance (GPU ^a)					Ideal gas selectivity		
	P/I _{N2}	P/I _{CH4}	P/I _{O2}	P/I _{CO2}	P/I _{H2}	$\alpha_{H2/N2}$	$\alpha_{CO2/CH4}$	$\alpha_{O2/N2}$
Blend membrane #1	2.7	3.3	14	46	153	57	14	5.2
Blend membrane #2	1.6	1.8	10	36	124	78	20	6.2
Blend membrane #3	0.6	0.7	2.9	14	61	102	20	4.8

^a1 GPU = 1x10⁻⁶ cm³(STP)/cm² s cmHg

To quantify chemical resistance, the mass of pure Matrimid and blended membranes that did not dissolve in several oxygenated aromatics was measured (Figure 3–12). An insoluble mass of 100% suggests that none of the membrane dissolved, while an insoluble mass of 0% means the membrane completely dissolved.

Some values were greater than 100% because NMP was used to push the last bit of solution from the head space of the filter. NMP was chosen because PBI falls out of

Table 3–9. The average spacing between polymer molecules and densities for pure films and blended membranes

Membrane	d-spacing (Å)	ρ (g/cm ³)
Matrimid dense film	4.3	1.254
50/50 PBI-Matrimid membrane	3.5, 5.2	1.284
PBI dense film	3.7	1.320

solution so easily. To remove the mass of dissolved polymer from the filter without it precipitating, a good solvent must be used to get a “worst case scenario” for how much PBI dissolved. Unfortunately, NMP has a high boiling point and upon heating for longer periods of time at 150°C, the filter melted, trapping the NMP inside before all of it had been removed. Error bars were determined by the amount of NMP that was likely to be left in the filter after heating the filter to remove the chemicals used to test chemical resistance. Even with these generous errors bars, stark differences between the

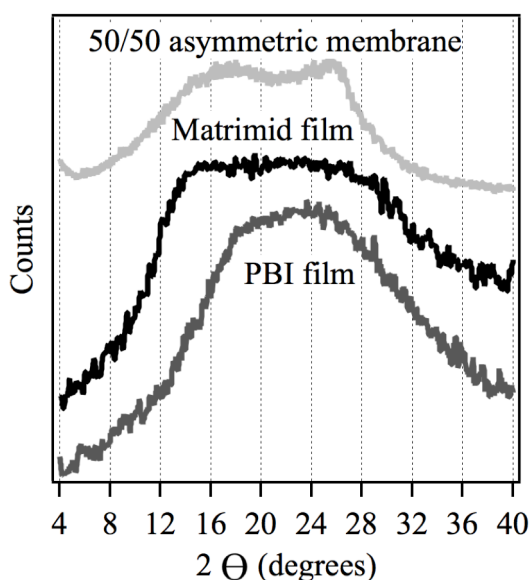


Figure 3–11. XRD spectra for a Matrimid film, a PBI film and a 50/50 PBI-Matrimid asymmetric membrane. All are amorphous in structure. The 50/50 blend spectra is similar to the 100 Matrimid film.

performance of the Matrimid and blend membranes is apparent and as a screening process, this procedure was deemed acceptable. In three of the four chemicals probed, the pure Matrimid membranes completely dissolved. In all cases, the 50/50 blend membranes were within the error bars of not dissolving at all. This suggests that the PBI is protecting the Matrimid from chemical attack or the PBI and Matrimid together are more resistant to chemical attack. This suggests that

the two polymers are well blended.

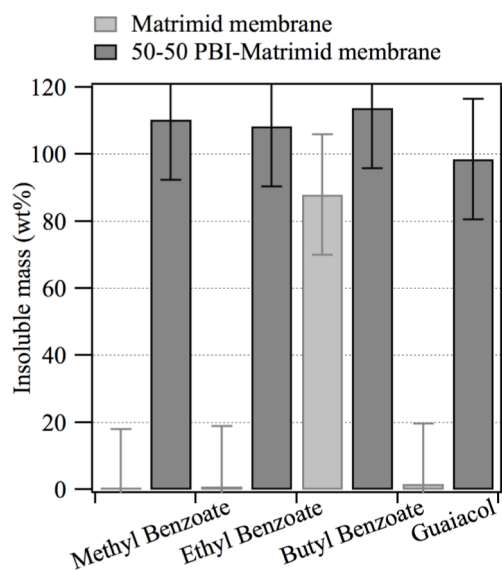


Figure 3–12. Blended membranes demonstrate greater resistance to chemical attack by selected oxygenated aromatics at 50°C for 18 hours.

4. Conclusions

Processes for making blended PBI-Matrimid dense films and asymmetric membranes have been reported. Films showed decreasing permeability and selectivity with increasing weight fraction of PBI. 50/50 PBI-Matrimid membranes were fabricated via phase inversion process with some membranes having the same selectivities of the dense films. Blended membranes were more stable to chemical attack by oxygenated aromatics than the pure Matrimid membranes suggesting membranes were blended. Membranes with significant thermal and chemical resistance may expand the use of membranes in applications at higher temperatures and in harsher chemical environments.

Chapter 4 - Thermal stability of PBI/Matrimid films and membranes

1. Introduction

Membranes with enhanced thermal and chemical resistance could expand the use of membranes in high temperature gas streams and as phase contactors or for product separation in membrane reactors. High temperature gas streams include H₂ from syn gas in gasification (>250°C)[62]. In membrane reactors with three phase systems, the membrane is used as a phase contactor between a liquid and gaseous reactant in order to maintain constant coverage of the gaseous reagent on the catalyst, which can have implications for reaction selectivity, and results in lower pressure operation, potentially reducing equipment costs and improving process safety[18,19].

Currently, there are few asymmetric polymeric membranes that maintain their selectivity and permeance at temperatures in the 200°C range. Commercially available reverse osmosis membranes, with polyamide separating layers, have been investigated for water and isopropanol separations up to 200°C[63]. The membranes performed best, with the largest fluxes and separation factors, at 150°C, but at 200°C there was a dramatic loss in flux and selectivity as the structure became much denser. Asymmetric polyaramide, polyimide, and polyimide on a polyetherimide support have been investigated at temperatures up to 220°C. The polyaramide displayed stable H₂/n-butane separations at 175°C[64]. Dense films of the polyimide 6FDA-TADPO, were found to have selectivities H₂/CH₄ of 40 at 200°C[65]. This work examines the potential for polyimide blend membranes to be used over extended periods at temperatures in excess of 200°C.

There are several requirements for a polymer that would be appropriate for fabricating an asymmetric membrane that can operate in this range. The polymer must have T_g above 300°C. There must also be appropriate solvents for asymmetric membrane fabrication. For economic reasons, the ideal membrane has large permeances and selectivities so that membrane area can be minimized. Finding one polymer that meets all of these requirements is difficult. Another option is to blend two polymers. By blending polymers, properties of the membrane can be tailored.

Polyimides (PI) and polybenzimidazoles (PBI) are logical polymers to examine because PIs and PBIs have T_g 's in the required range. Table 4–1 shows Matrimid 5218, referred to as Matrimid from here on, and a PBI. Matrimid is considered a more attractive material than PBI for fabricating a gas separation membrane because Matrimid is at the boundary of Robeson's upper bound. Matrimid has a larger H_2 permeability, 27 Barrer versus 0.6 Barrer, and approximately the same α_{H_2/N_2} as PBI[47]. Transport can be described in blends by the following empirical model

$$\ln P_{blend} = \phi_1 \ln P_1 + \phi_2 \ln P_2 \quad (22)$$

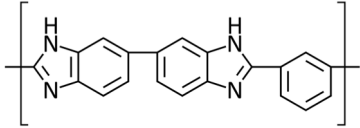
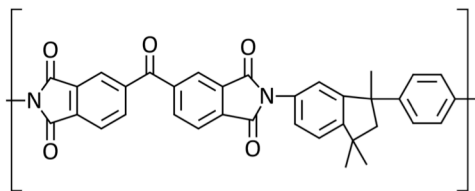
where P_{blend} is the permeability of the blend composed of polymer 1 and 2, ϕ is the volume fraction of the polymers, and P is the permeability of the polymers.

PBI has a T_g of 435°C and considerable chemical resistance[66]. Matrimid has a high T_g , 320°C, and good chemical resistance, although less than PBI[67]. Fox's equation is used to predict the T_g of a blend

$$\frac{1}{T_{g,blend}} = \frac{w_1}{T_{g,1}} + \frac{w_2}{T_{g,2}} \quad (23)$$

based on the weight fractions of polymer 1 and 2, w_1 and w_2 , and T_g of each polymer. This equation predicts that a membrane fabricated with equal parts PBI and Matrimid should have a T_g of approximately 350°C and therefore by rough estimate, this blend could demonstrate stable permeance at 300°C[68]. Asymmetric membranes must be operated at temperatures below the T_g of the membrane because at temperatures close to the T_g the substructure collapses, lowering both permeances and selectivity[68]. We have previously demonstrated the ability to fabricate integrally skinned flat sheet asymmetric membranes from these materials in Chapter 3.

Table 4–1. Properties of a PBI and Matrimid 5218

Polymer	Repeat unit structure	T _g ^a (°C)	Density (g/cm ³)	Average d-spacing (Å)	Frac. Free Vol. ^b
PBI		435	1.320	3.7	0.145
Matrimid 5218		320	1.254	4.3	0.191

^aFrom reference [66] ^bOccupied volume calculated via group contribution[56]

The goal of this research is to characterize the properties of a blended polymeric membrane at conditions above ambient conditions to expand of the conditions where polymeric gas separation membranes can operate, enabling new gas separation and membrane reactor applications.

2. Experimental

2.1 Materials

Reagent grade chemicals were purchased from Sigma-Aldrich and Cole Parmer. PBI (100 mesh powder) was obtained from PBI Performance Products (Charlotte, NC, USA). Matrimid was obtained from Archway Sales (Kansas City, MO, USA). Gases were obtained from Matheson TRIGAS and had a purity of at least 99.98%. All supplies were used as received.

2.2 Dense films and asymmetric membranes

The procedure for fabricating blended dense films of PBI and Matrimid is found in Chapter 3. Membranes were made with PBI/Matrimid ratio of 50/50. The general procedure is found in Chapter 3. Membranes were cast 350µm thick on a glass plate and underwent 15 seconds of forced evaporation before being quenched in a bath of DI water (T = 12°C) for 24 hours.

2.3 Characterization methods

2.3.1 Gas transport measurements

Single gas permeabilities for dense films and asymmetric membranes were measured using a constant volume-variable pressure system with an oven[49]. Measurements were taken at a feed pressure of 10.2 atm gauge. The error due to the leak rate was less than 10% for the slowest gas in the film with the smallest permeability.

2.3.2 Chain packing

A Rigaku Miniflex II (Japan) X-ray diffractometer (XRD) with Cu K α radiation source was used to investigate the arrangement and chain spacing of polymer molecules. The average d-spacing between polymer chains was calculated using Bragg's law:

$$n\lambda = 2d\sin\theta \quad (24)$$

where n is an integer, λ is the wavelength of the x-ray, d is the spacing between polymer chains and θ is the diffraction angle.

2.3.3 Thermal stability

Decomposition with temperature was quantified using a Perkin Elmer Pyris 1 thermogravimetric analyzer (TGA) (Norwalk, CT). About 5 mg of sample was placed in a pan. Samples were heated from room temperature to 100°C at 25°C/min. Sample was held at 100°C to desorb water and then heated from 100 to 620°C at 10°C/min.

3. Results and discussion

3.1 Dense blend PBI/Matrimid films

Permeabilities of N₂, CH₄, O₂, CO₂ and H₂ were measured from 21 to 200°C for films with 25/75 and 50/50 PBI/Matrimid. In all cases, the permeability of gases in order of slowest to fastest was CH₄, N₂, O₂, CO₂, and H₂, although at 150 and 200°C, CH₄ and N₂ had identical permeabilities. Films with more Matrimid had larger permeabilities. PBI has a lower FFV than Matrimid which results in PBI having smaller permeabilities.

Selectivities for three gas pairs from 21 to 200°C, H₂/N₂, CO₂/CH₄, and O₂/N₂, are shown in Figure 4–1. The ideal selectivities of the blend films decreased with increasing temperature. Selectivity is determined by diffusive selectivity and sorption selectivity. Diffusive selectivity becomes smaller with increasing temperatures because diffusion typically increases more for the slower gas. Sorption selectivity also becomes smaller as all gases have lower sorption at higher temperatures. Increasing the wt% PBI from 25 to 50 wt% does not have any effect on selectivity.

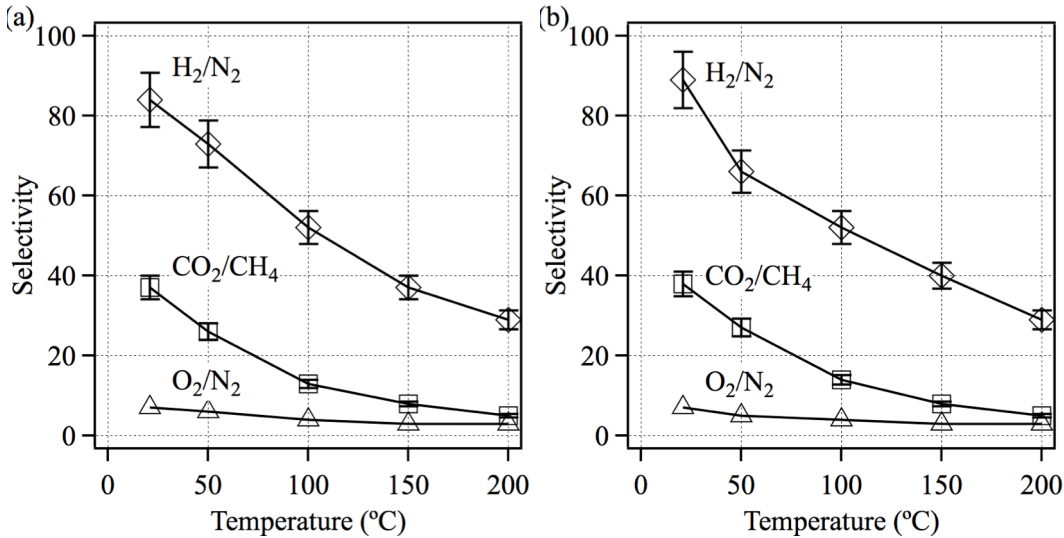


Figure 4–1. Ideal selectivities for several industrially important separations of blended dense PBI/Matrimid films a) 25/75 b) 50/50. Line added to guide the eye.

The transport process can be described as an activated process with the van't Hoff-Arrhenius equation:

$$P = Ae^{E_P/RT} \quad (25)$$

where P is the permeability, A is the pre-exponential factor, E_P is the activation energy for permeation, R is the gas constant, and T is the temperature. Figure 4–2 shows the Arrhenius plots for 25/75 and 50/50 films. Calculated values of the activation energy for permeation are reported in Table 4–2. The PBI/Matrimid blends have activation energies that are approximately 50% of the value for pure Matrimid films. Smaller activation energies indicate that an increase in temperature results in only a modest increase in flux, probably because the polymer chains are rigid and remain so as temperature increases. This suggests that adding a small amount of PBI to the polymer markedly reduces the resulting chain mobility. After adding a small amount of PBI, adding more PBI does not result in a more rigid structure. This is promising because

permeabilities of 50/50 blends are closer to pure Matrimid than pure PBI. Matrimid has much more desirable gas transport properties than PBI. Adding a small amount of PBI enhances the ability of the film to remain rigid at elevated temperatures but without a significant loss in permeability.

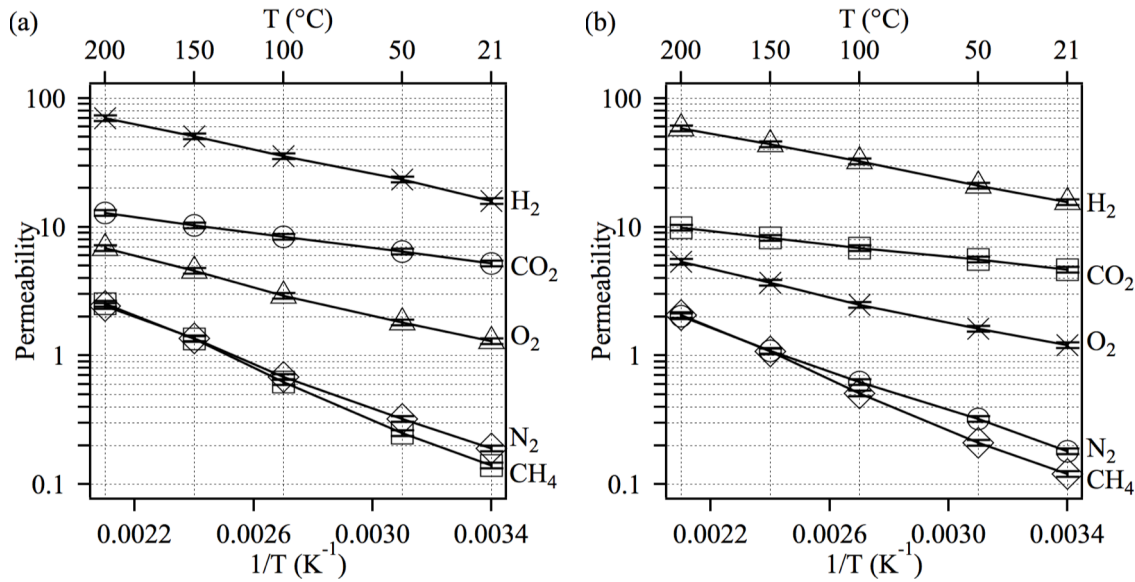


Figure 4–2. PBI/Matrimid blended dense films have linear relationships between $\ln(\text{Permeability})$ and $1/T$ ($1/\text{K}$) from 21 to 200°C (a) 25/75 PBI/Matrimid film (b) 50/50 PBI/Matrimid film

Table 4–2. Activation energy for permeation for gases in blended PBI/Matrimid films

Sample	E_{p,N_2} (kJ/mol)	E_{p,CH_4} (kJ/mol)	E_{p,O_2} (kJ/mol)	E_{p,CO_2} (kJ/mol)	E_{p,H_2} (kJ/mol)
100 Matrimid	27.2	32.5	-	10.0	-
25/75 PBI/Matrimid	16.4	18.8	10.6	5.7	9.4
50/50 PBI/Matrimid	15.6	18.6	9.6	4.8	8.6

^a[85] Temperature range from 35-308°C

3.2 50/50 PBI/Matrimid asymmetric membranes

Permeance and selectivity are two critical characteristics of gas separation membranes. Permeances of N₂, CH₄, O₂, CO₂ and H₂ in a 50/50 blend membrane from room temperature to 200°C are presented in Figure 4–3. For each gas, fluxes were higher at 50°C than room

temperature. Flux increases with temperature because polymer chains are more likely to have the energy to move. More movement increases the chance a gas molecule will successfully complete

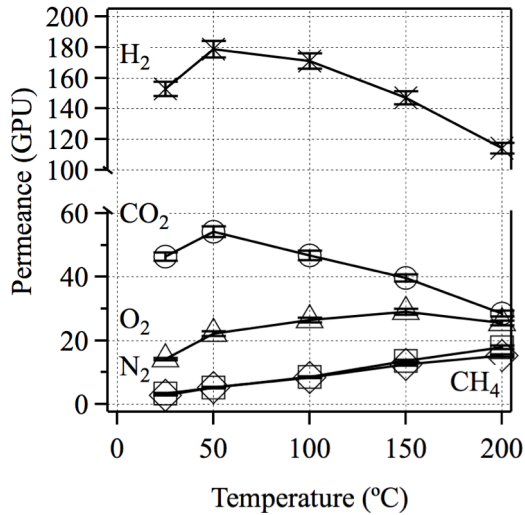


Figure 4–3. The slow gases, CH₄ and N₂, have larger permeances with increasing temperature while the fast gases, H₂ and CO₂, show a maximum permeance at 50°C in 50/50 PBI/Matrimid asymmetric membranes. Line added to guide the eye.

reduction in gas flux for H₂ and CO₂ is the result of either substructure collapse or skin densification. The fast gases need a substructure with less resistance to allow the skin layer to control transport [11].

In all cases, selectivity falls as temperature increases (Figure 4–4). Selectivity decreases with increasing temperatures because of the inherent properties of the polymers and because of the increased resistance of the substructure[69]. At 200°C, the membrane has a selectivity of 7.5 for H₂ over N₂, 1.6 for CO₂ over CH₄ and 1.7 for O₂ over N₂.

a diffusive jump in the polymer matrix, increasing the rate of diffusion of gas molecules[62]. Above 50°C, the permeances of slow gases continue to increase up to 200°C. O₂ has the same permeance from 100°C to 200°C, while the fast gases CO₂ and H₂ have lower permeances at 200°C than 50°C. As the polymer permeabilities are continually increasing over this temperature range (Figure 4–2), the

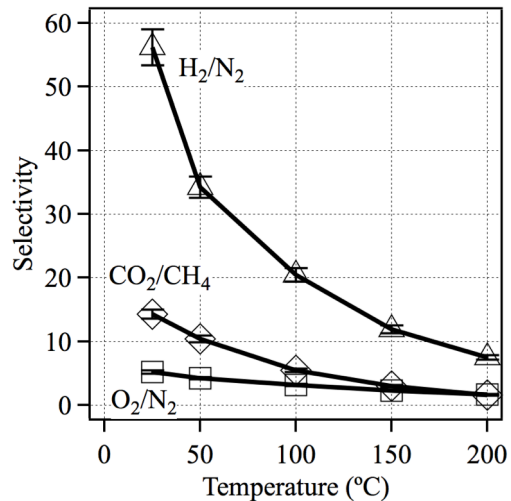


Figure 4–4. Pure gas selectivities of a 50/50 PBI/Matrimid membrane for several commercially important processes are shown. Line added to guide the eye.

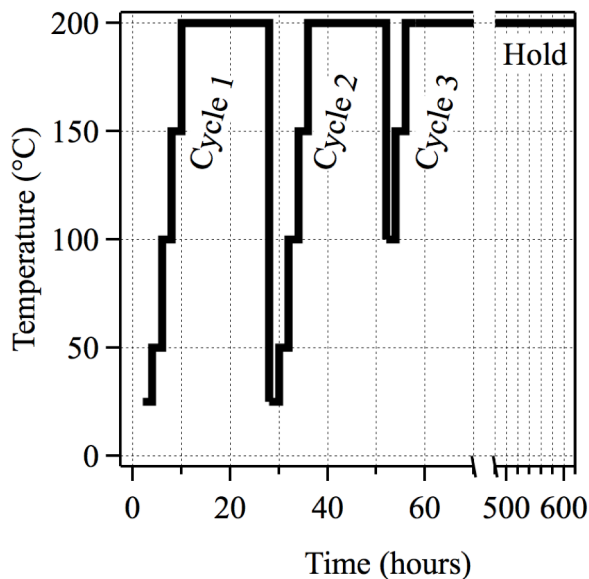


Figure 4-5. The thermal stability of asymmetric membranes was determined by cycling the membrane from room temperature to 200°C. Each time the temperature changed, permeance was measured.

was determined to be stable at the elevated temperature it was held at this temperature for 45 days to determine the long-term stability of the membrane.

3.2.1 Stability of 50/50 PBI/Matrimid at 200°C

The thermal integrity of the membrane for short periods of time was determined by measuring gas fluxes at discrete temperatures before and after annealing for 18 hours at some elevated temperature, either 200 or 300°C. Figure 4-5 shows the temperature ramp for the 200°C tests. For the membranes annealed at 200°C, gas fluxes were measured at room temperature, 50, 100, 150 and then 200°C. The membrane was then held at 200°C for 18 hours and then allowed to cool back to room temperature and fluxes were again measured at room temperature, 50, 100, 150 and 200°C. This process was repeated twice and then if the membrane

Gases generally had lower permeances after the first annealing process but showed little additional loss following the second annealing process (Figure 4–6). Lower permeances could be the result of a densification of the skin layer or the substructure or a combination of the two. The

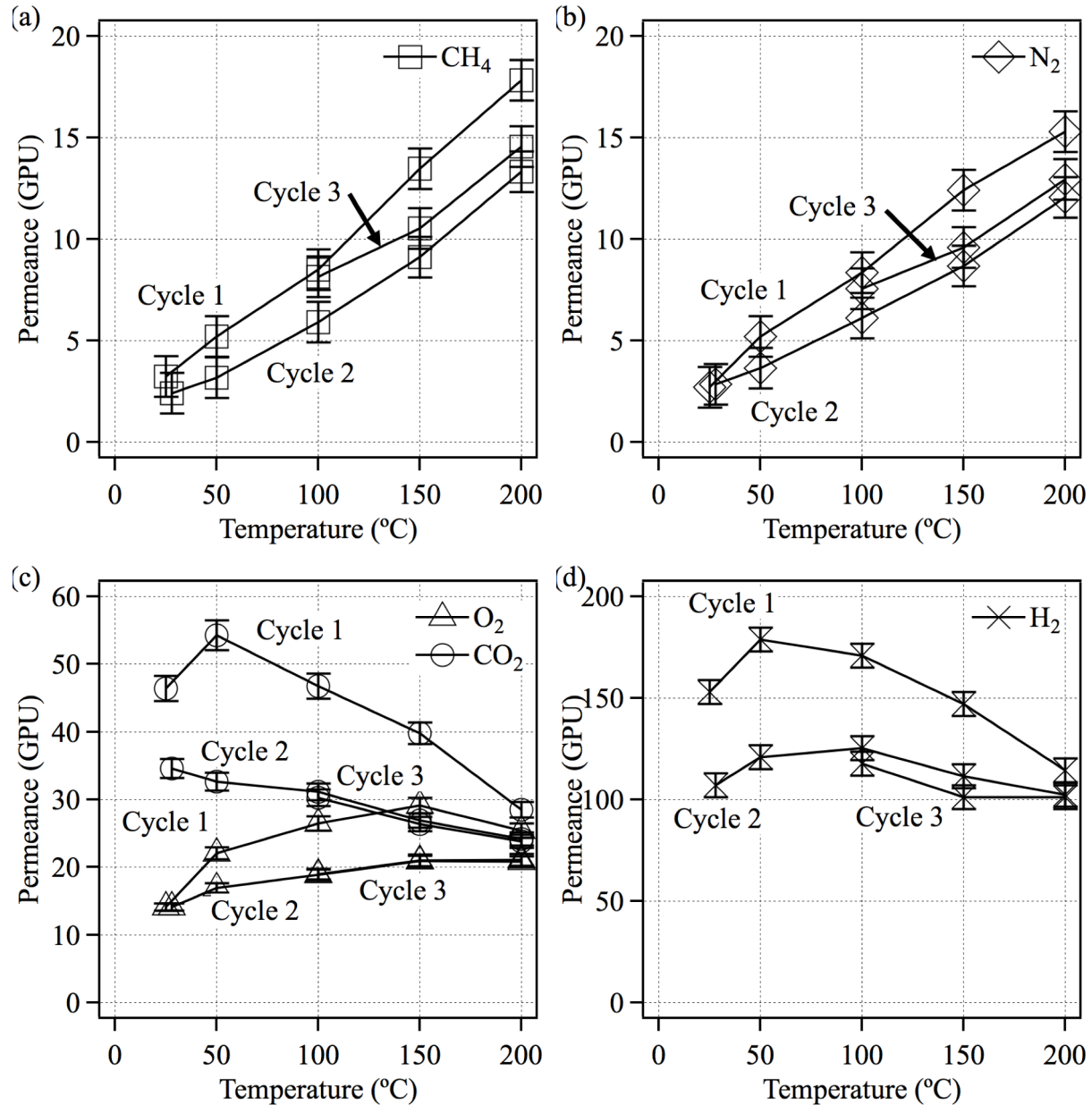


Figure 4–6(a-d). Permeance falls from cycle one to cycle two but not between cycle two and three suggesting that the membrane is stable after the first annealing cycle.

substructure consists of a network of pores which have a high free energy. As such, the pores are more thermodynamically unfavorable than a dense, nonporous structure, and are susceptible to

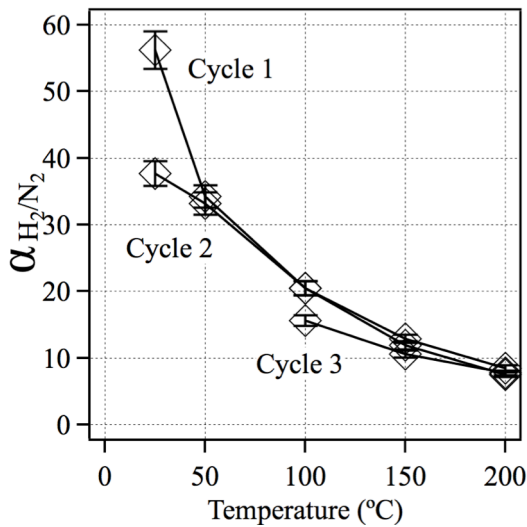


Figure 4–7. Selectivity changes little between cycles. Line added to guide the eye.

α_{H_2/N_2} changed from 8 to 5.

The densification of the substructure is responsible for the decrease in permeance of fast gases at temperatures above 50°C. To investigate this, another membrane with known permeance and selectivity was heated to 200°C for 48 hours. After this process, the permeance was tested again. Then, the selective skin layer was carefully removed with a fine grain sand paper. This process was repeated several times. For comparison, an unannealed membrane was also tested and the skin layer

collapse. Pore collapse in the substructure would result in resistance to transport in both the substructure and the skin layer, lowering permeances[11,69]. Selectivity was stable in all three cycles (Figure 4–7).

Because the membrane appeared stable, the membrane was tested on longer time scales. N_2 and H_2 flux and selectivity of the membrane for these two gases kept at 200°C for 45 days under air when not being tested are shown in Figure 4–8. The membrane maintained similar levels of gas flux and selectivity. Hydrogen fluxes changed from 101 to 81 over this time while

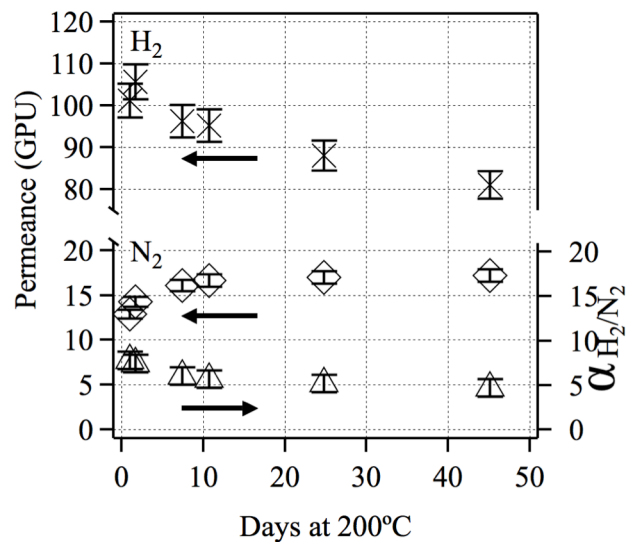


Figure 4–8. N_2 flux and selectivity are constant between 10 and 45 days at 200°C in an air environment.

removed in the same fashion. The permeance and selectivity as a function of number of sandings for both membranes can be found in Figure 4–9.

The membrane that was not annealed had drastic changes in permeance with only a few sandings. The N₂ and H₂ permeances before sanding were 0.4 and 6.8 GPU, respectively, and α_{H_2/N_2} was 17. This suggests the skin layer is on the order of 1 μm thick with few defects. After four sandings, the permeances of both gases have increased by four orders of magnitude and the selectivity is approaching that of convective flow. Thus almost all of the resistance to transport in the unannealed membranes is found in the skin layer and not in the substructure.

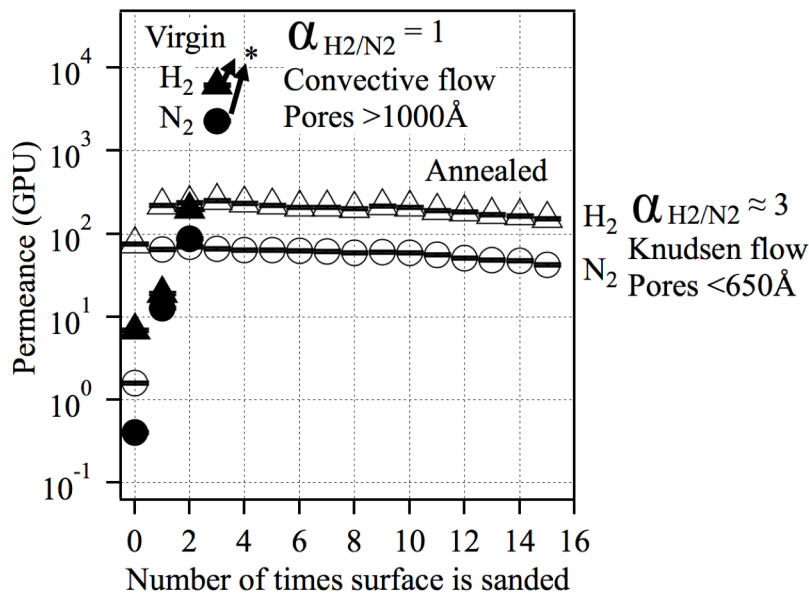


Figure 4–9. The resistance to transport due to the substructure of an unannealed and an annealed membrane was investigated by removing membrane material with a sheet of fine grain sandpaper. The unannealed (virgin) membrane had selectivities below Knudsen diffusion after one sanding suggesting the substructure has little resistance to transport. The annealed membranes had Knudsen diffusion selectivity after 15 sandings, suggesting the substructure has significant resistance. (*After the fourth sanding of the virgin membrane, the gas flux exceeded the capacity of the test system.)

The annealed membrane had less drastic changes in permeance with sanding. Before annealing, the membrane had N₂ and H₂ permeances of 2.4 and 124.6 GPU, respectively, and

α_{H_2/N_2} was 52. Compared to the membrane that was not annealed, this membrane has a thinner (~0.2 μ m) and more defect-free skin layer, although it is not entirely free of defects. After annealing, the permeances were lower, 1.6 and 75 GPU for N₂ and H₂, respectively, as was α_{H_2/N_2} (47 after annealing versus 52 before annealing). This drop in both permeances and selectivity is similar to the membrane tested in Figure 4–3 in that, after annealing at 200°C for 18 hours, both the flux and selectivity decreased. After a single sanding, the membrane's H₂ and N₂ permeances increased by 3 and 40 times, respectively. The resultant selectivity was that of Knudsen diffusion. Subsequent sandings, up to 14 sandings, resulted in no measurable change in selectivity and a small reduction in flux. The slow drop in permeances might be due to the deposition of fine particles from the sanding process in the membrane with repeated pressurizations with flux measurements. There might also be a gradient in resistance to transport in the substructure. After annealing, the entire substructure has significantly more resistance to transport. An increase in the resistance to transport in the substructure is associated with a decrease in selectivity of a membrane because the resistance to transport in the substructure results in a decrease in the permeance of the faster gas[69].

3.2.2 Stability of 50/50 PBI/Matrimid at 300°C

With the proven stability of the membrane at 200°C, the same temperature ramp experiment found in Figure 4–5 was repeated, this time testing permeance from room temperature to 300°C. The same 18 hour annealing period was performed but at 300°C instead of 200°C.

Changes in fluxes and selectivities were more dramatic with annealing at higher temperatures (Figure 4–10). Permeances in the second cycle were much smaller than the permeances in first cycle. For instance, H₂ permeances at room temperature after annealing at 300°C were only 3% of their pre-annealing levels. Selectivities were less than 20% of pre-annealed α_{H_2/N_2} at room temperature; however, at 200 and 300°C the membrane has a separation factor almost identical to that of a dense film after annealing. A decrease in both flux and selectivity is the result of an increase in density in the porous substructure and the dense skin layer[68]. There appears to be no change in either permeance or selectivity after the first cycle, suggesting that after 18 hours at 300°C, the structure is no longer changing with successive heating cycles.

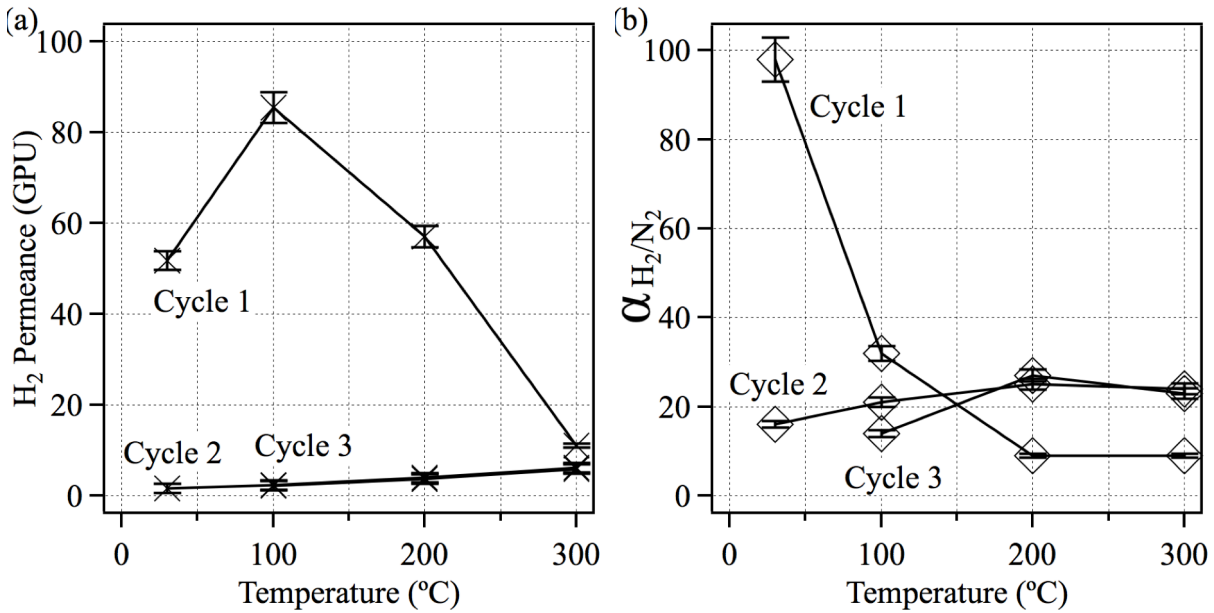


Figure 4–10. To test the stability of 50/50 PBI/Matrimid membranes at 300°C, the same temperature ramp experiment found in Figure 4–5 was performed, this time to 300°C. Membranes were held at 300°C for 18 hours in between cycles. (a) At all temperatures, H₂ permeances were smaller after annealing at 300°C. (b) α_{H_2/N_2} at 200 and 300°C are higher after annealing at 300°C for 18 hours. After a second heating and annealing cycle, selectivities change little. Lines added to guide the eye.

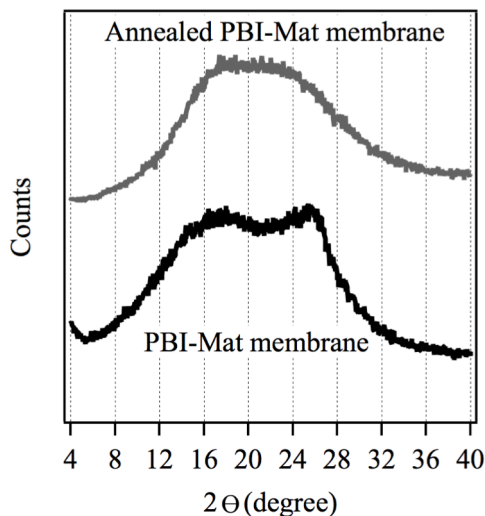


Figure 4–11. Thermal annealing of membrane changes the distribution of spacing between polymer chains.

3.2.3 Properties of 50/50 PBI/Matrimid membranes annealed at 200°C

The rest of the paper discusses properties of membranes annealed at 200°C. Annealing changes several properties of the membrane (Table 4–3). The membrane is denser after annealing. While the average d-spacing between polymer molecules is essentially

unchanged after annealing, shifting from 4.3 to 4.4Å, the distribution of spacings between molecules does change (Figure 4–11). Before annealing, two distinct spacings at 3.5 and

5.2Å are present while after annealing there is one most common spacing.

Another way to quantify thermal resistance is by measuring the mass of membrane remaining as the sample is heated (Figure 4–12). Membranes that were annealed retained more mass than the untreated membrane at the same temperature in both N₂ and air (Table 4–4).

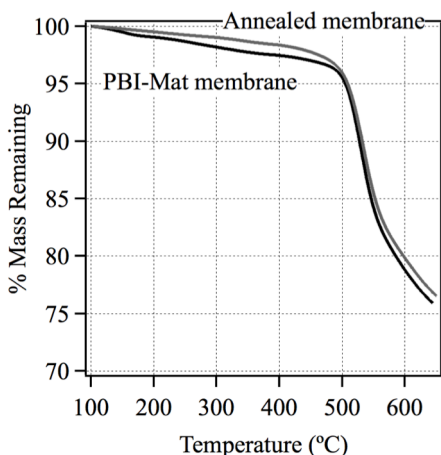


Figure 4–12. The mass remaining

Table 4–4. 50/50 PBI/Matrimid membranes are more stable with respect of temperature than pure Matrimid.

Sample	Temperature at 5% weight loss (°C)		Residual mass at 620°C	
	N ₂	Air	N ₂	Air
50/50 PBI/Matrimid membrane	530	505	80	78
Annealed 50/50 PBI/Matrimid membrane	540	510	81	78

Table 4–3. Properties of blended membrane samples before and after heat treatment

Sample	Density (g/cm ³)	Average d-spacing (Å)
PBI/Matrimid membrane	1.284	4.3
Annealed PBI/Matrimid membrane	1.311	4.4

4. Conclusions

Blends of PBI and Matrimid films and membranes have been tested across a range of temperatures. Films demonstrate adding a small amount of PBI results in a more rigid structure. Increasing the wt% PBI from 25 to 50% does not result in a significantly more rigid structure. 50/50 blend asymmetric membranes were tested from room temperature to 300°C. The membranes have stable

permeances at 200°C after annealing for 18 hours at 200°C; however, there is a densification of the substructure which results in undesirable drop in permeance at temperatures above 100°C. For membranes annealed at 300°C, the fluxes are significantly lower, but selectivity of the membrane for H₂/N₂ at 200°C, 23, was close to

that of a dense film, 29. The polymer is stable to 200°C but membranes see an increase in substructure resistance at temperatures above 100°C resulting in an undesirable drop in both permeance and selectivities at temperatures above 100°C.

There are several ways to mitigate this undesirable substructure collapse, including adding a crosslinking agent to the existing dope or making a composite membrane from two different materials. Adding a crosslinking agent, and then curing it, either chemically or thermally, would result in a tighter substructure that could be more resistant to collapse. Crosslinking often results in smaller permeances, but larger selectivities. Another way to avoid pore collapse in the substructure, without crosslinking, is to make the skin layer and the substructure separately, from different materials. This way, the substructure could be made with a more thermally resistant material, such as a ceramic, and a thin, polymeric skin layer could be deposited on the ceramic.

These blend membranes could extend the use of membranes in several applications. For existing operations, because permeances are higher at elevated temperatures, it might be economical to perform some separations at higher temperatures. Other applications where membranes are not yet used but could be if they were stable at higher temperatures include the separation of CO₂ from pre-combustion gases for carbon capture where temperatures are in excess of 250°C. Another application that requires chemically and thermally stable membranes are membrane reactors. Membrane reactors compete with more traditional reactors such as packed-bed and slurry reactors. In both of these traditional technologies, it is unlikely that the nature of the reactor determines the thermal limits of the reaction. For polymeric membrane reactors, the thermal stability of the polymer is likely to be a consideration in the design of a reactor. By fabricating a more thermally stable membrane, we have increased the range in which polymeric reactors can compete with these traditional technologies.

Chapter 5 - Mild solvent post treatments of blended asymmetric PBI/Matrimid membranes

1. Introduction

The separating layer of gas separation membranes is required to be thin, for large permeances, but defect-free, because a small area of defects drastically reduces the ability of the membrane to produce streams enriched one component or another. Producing both thin and defect-free separating layers in asymmetric membranes represents a challenge for the membrane industry because the thinner the skin layer is, the increasing likelihood of defects.

There are several strategies for mitigating the harmful effects of defects in the separating layer. The most commonly employed method, developed by Henis and Tripodi, involves coating the separating layer with a thin layer of a moderately selective but highly permeable polymer. This layer improves the selectivity of the original, defective skin layer by drastically reducing the amount of material that passes through the defect[11,12]. Other post-treatment strategies to improve selectivity of gas separation include the use of UV-radiation, ammonia gas, fluorination, plasma, and ozone to modify the skin layer[58,70–73].

Others have explored liquid and vapor treatments of asymmetric membranes with dense skin layers for liquid or gas separations. It has been noted that cellulose acetate membranes see improvements in selectivity in pervaporation experiments for methanol and methyl tert-butyl ether (MTBE) separations when soaked in an aqueous bath with one of the following compounds; acetone, dioxane, and ethanol[74]. Treating the polyamide separating layer of a reverse osmosis membrane resulted in small increases in He/N₂ selectivity, although not for O₂/N₂ selectivity[75]. Others have investigated several liquid treatments of polyetherimide membranes to improve selectivity in gas separations[76]. Rezac et al. investigated liquid and vapor treatments of polysulfone, polyimide, and phenylene oxide on ceramic supports, with dichloromethane, cyclohexane and water[77].

In this paper, integrally skinned asymmetric membranes made of two different polymers, a commercially available polybenzimidazole (PBI) and Matrimid 5218, referred to as Matrimid in the rest of the paper, are explored. Both vapor and liquid post-treatments to improve selectivity are explored. The chemical structure of these two polymers can be found in Figure 5–

1. To our knowledge, there has not been any exploration of liquid and vapor post-treatments of blend membranes to improve selectivity for gas separation purposes.

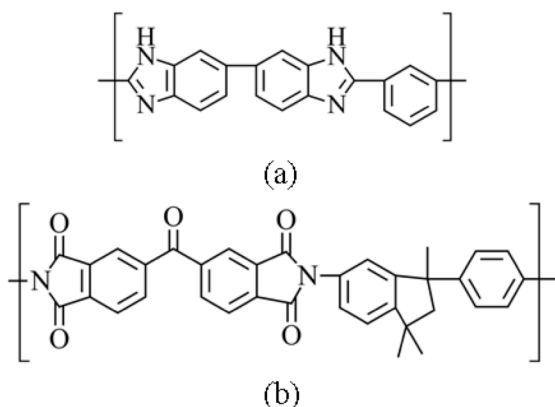


Figure 5–1. Chemical structure of a) PBI and b) Matrimid 5218

Products (Charlotte, NC, USA). Matrimid was obtained from Archway Sales (Kansas City, MO, USA). Ultra high purity gases were obtained from Matheson TRIGAS and had a purity of at least 99.98%. All supplies were used as received.

2. Experimental

2.1. Materials

Reagent grade chemicals were purchased from Sigma-Aldrich and Cole Parmer. PBI (100 mesh powder) was obtained from PBI Performance

2.2 Fabrication of asymmetric PBI-Matrimid membranes

Asymmetric membranes were prepared by the Loeb-Sourirajan phase inversion process[10].

2.3 Vapor post-treatments of asymmetric PBI-Matrimid membranes

Vapor treatments were applied to only the skin side by placing the membrane in a Millipore cell. The side of the cell with the porous side of membrane was capped. The side of the cell with the skin side of the membrane was connected to an Erlenmeyer flask containing the treatment. For each treatment, membranes were left in the cell for 30 minutes.

2.4 Liquid post-treatments of asymmetric PBI-Matrimid membranes

Liquid post-treatments were applied with a sponge dipped in the treatment and then dragged in two half circles across the selective skin layer, not touching the edges of the membrane, but completely wetting the surface. If the treatment touched the porous substructure, the membrane curled and was not useful for further study. The liquid was left on the surface of

the membrane for approximately five minutes before the membranes were placed in a vacuum oven at 60°C overnight to ensure complete removal of the treatment.

2.5 Measuring transport properties

Single gas permeation of asymmetric membranes was measured using a constant pressure-variable volume system. Measurements were performed at a differential pressure of 3.4 atm with a membrane area of 13.8 cm² at a temperature of 25°C.

2.6 Data analysis

Statistical analysis was performed with SAS. Tukey-Kramer method was used to determine differences in treatments. It was concluded that there was evidence for treatment differences if p-values were less than 0.05, or a 95% confidence level. This confidence level was chosen because Type I errors, where the null hypothesis was rejected, but was in fact true, were determined to be more grievous than Type II errors. If the null hypothesis was incorrectly rejected, the incorrect conclusion, that there are differences between the treated and the control membranes, would be drawn. This additional treatment, if implemented, would require significant expense. A Type II error, where the conclusion fails to reject the null hypothesis, while it is true, is less grievous. If the experiment fails to determine a difference between the treated and untreated membranes, the recommendation would be to not add an additional treatment step to these membranes and the outlay of cost would not occur. Because Type I and Type II errors are inversely related, a 95% confidence level, with a lower risk of a Type I error than a lower confidence level, was determined to be best.

3. Results and discussion

3.1 Selection of treatments

Rezac et al. proposed that defects, or pores, are eliminated in a two-step process[77]. First, the liquid swells the polymer matrix, decreasing the modulus, and bringing the polymer chains surrounding the defect closer together. Then, when the liquid evaporates, capillary pressure forces result in the elimination of the defect as the polymer chains collapse together. The size of defect that can be eliminated from a polymer matrix can be determined if the polymer modulus of swollen matrix can be determined. The polymer modulus can be estimated

from the glass transition temperature (T_g) of the swollen polymer matrix. In order to determine T_g of the swollen polymer matrix, the equilibrium volume fraction of liquid in the polymer matrix must be known. Equilibrium swelling data can be found for a number of pure polymers but data is considerably more rare for polymer blends[78–81]. As such, treatments were chosen in another way.

Solubility parameters can be used to predict polymer-solvent interactions. The solubility parameter, δ , defined as

$$\delta = \sqrt{CED} \quad (26)$$

where the CED is cohesive energy density, or the increase in internal energy required to eliminate all the intermolecular forces per mole of a substance. Solubility parameters can be represented as either one number, the Hildebrand solubility parameter, or it can be split into three components, the Hansen solubility parameters, accounting for the contributions of dispersion or van der Waals (δ_d) and polar interactions, (δ_p), and hydrogen bonding, (δ_h), to the solubility component[82,83]. The dispersion component is due to temporary unequal electron distributions in the compound. The polar component is due to more permanent unequal electron distributions. The hydrogen bonding component is due to the presence of a hydrogen atom attached to an electronegative atom such as oxygen or nitrogen. For this work, Hansen solubility parameters were used.

For one substance to dissolve or swell another, it must be similar in chemical nature (the principle of “like dissolves like”). If the dispersion, polar and hydrogen bonding solubility parameters are close, it is likely the component will dissolve another component. One way to estimate the relative goodness of a compound as a solvent is the calculate the difference between parameters using the following equation

$$\delta_{1-2} = \sqrt{(\delta_{d,1} - \delta_{d,2})^2 + (\delta_{p,1} - \delta_{p,2})^2 + (\delta_{h,1} - \delta_{h,2})^2} \quad (27)$$

Table 5–1. Calculated Hansen solubility parameters for polymers, NMP and chosen treatments.

	δ_d (MPa ^{1/2})	δ_p (MPa ^{1/2})	δ_h (MPa ^{1/2})
PBI	25.67	8.11	4.53
Matrimid	8.36	11.65	22.8
NMP	19.5	17.4	11.3
Pentane	14.4	0	0
2-Butanone	14.1	9.3	9.5
Ethanol	12.6	11.2	20

For Matrimid and PBI, the three solubility components were calculated from group contribution, while for chemical treatments, the parameters were found from tabulated data (Table 5–1)[56]. The three chosen treatments and Matrimid and PBI can be found on Figure 5–2. NMP, a known solvent for both components is also included for reference. In general, ethanol will act most like a solvent/swelling agent for Matrimid, while 2-butanone and pentane will act less so. For PBI, 2-butanone will act most like a solvent/swelling agent, while ethanol and pentane will act less so.

3.2 Vapor post-treatments

Vapor post-treatments were performed with pentane, 2-butanone and ethanol (Figure 5–3). Almost all pentane membranes saw larger improvements in

where 1 is the polymer and 2 is the solvent. While there is no rule for what number δ_{1-2} must be below for dissolution to occur, in general, the larger the number, the less one component will dissolve in the other. Another way to rank the ability of a compound to act like a solvent is to plot points on a graph and determine which components are closest to the polymer.

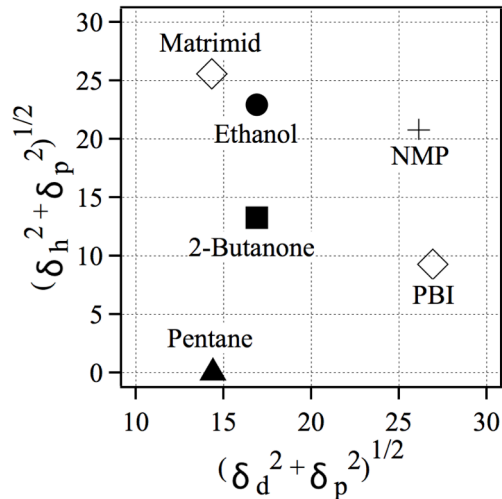


Figure 5–2. Matrimid and PBI points were calculated from group contribution while ethanol, 2-butanone, pentane and NMP were from tabulated data[56]. NMP is a known solvent for both Matrimid and PBI and is on the graph for reference. In general, ethanol should act more like a swelling agent for Matrimid while pentane will not. In general 2-butanone should act most like a swelling agent for PBI while ethanol and pentane are unlikely to have much effect.

selectivity than the measurement error. In other treatment groups, some membranes improved, while other membranes in each treatment group did not. Control membranes, which were dried and whose gas transport properties were measured with the treated membranes, had selectivities

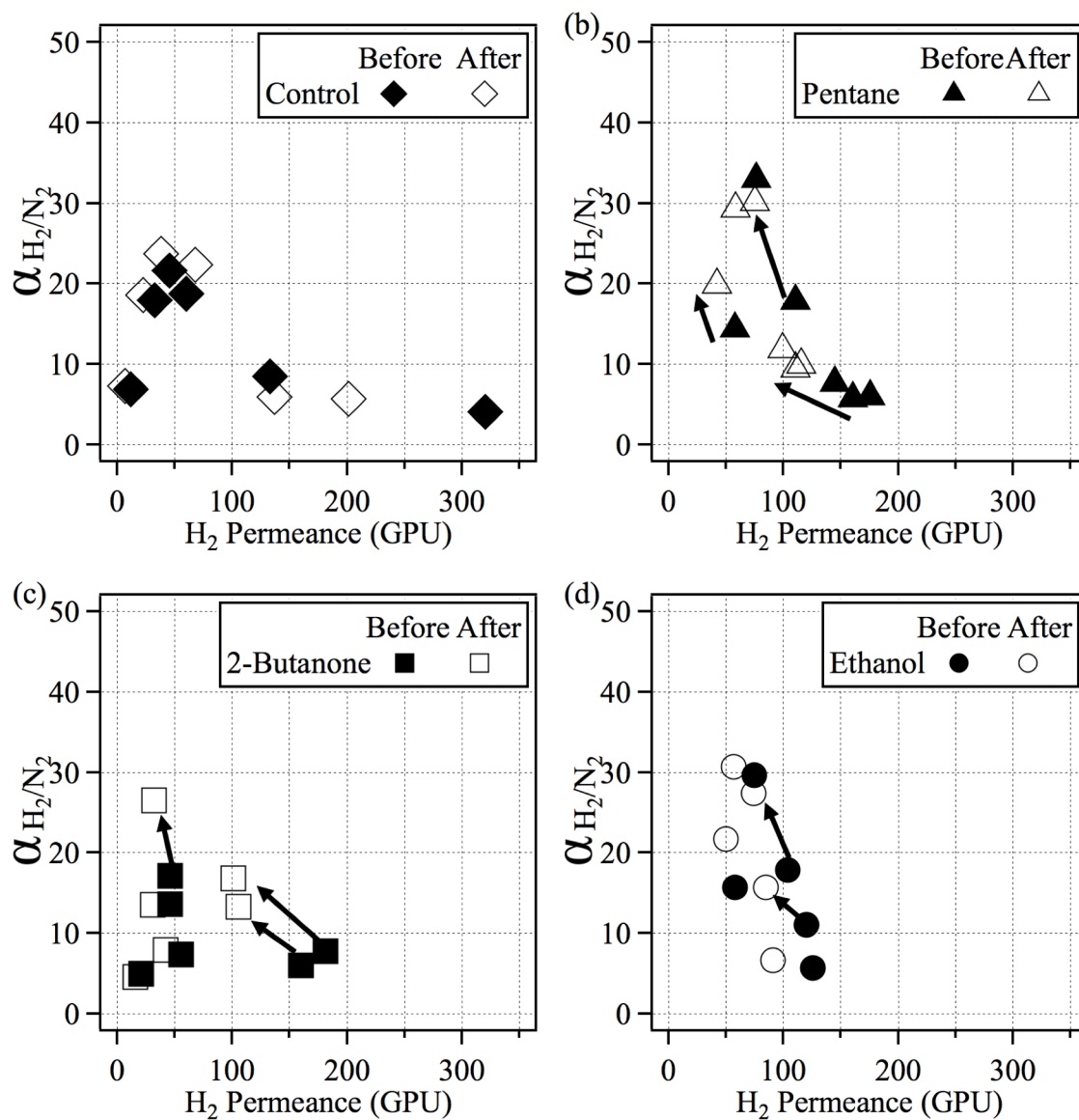


Figure 5-3. After one vapor treatment, almost all membranes treated with pentane were more selective. For those membranes treated with 2-butanone and ethanol, some membranes were more selective while others were not. Measurement error is the size of the points. (a) Selectivities of control membranes did not change (b) Pentane treatment (c) 2-butanone treatment (d) Ethanol treatment

within the measurement error. The control membrane with the largest permeance and lowest selectivity saw a significant drop in permeance, but no change in selectivity suggesting that the heating process to ensure removal of treatments has no effect on selectivity. In the 2-butanone groups; treated membranes with selectivities below 15 and permeances less than 50 GPU did not see improvements in selectivity with one treatment. Membranes with smaller fluxes and moderate selectivities have thicker skin layers than membranes with larger fluxes and higher selectivities. In these cases, perhaps significant amounts of the vapor treatment are not penetrating the full thickness of the skin layer and only defects on the surface layer are affected.

Almost all treated membranes that saw significant improvements in selectivity had smaller permeances, which suggests smaller or fewer defects. Almost all treated membranes that did not see significant improvements in selectivity had no significant change in permeance, suggesting the skin layer is unaffected by these treatments.

The effect of successive treatments on permeance and selectivity can be found in Figure 5–4. All control membranes had permeance and selectivity measurements within measurement error between treatment one and treatment three. For membranes exposed to a vapor, some membranes had lower permeances and higher selectivities with successive treatments.

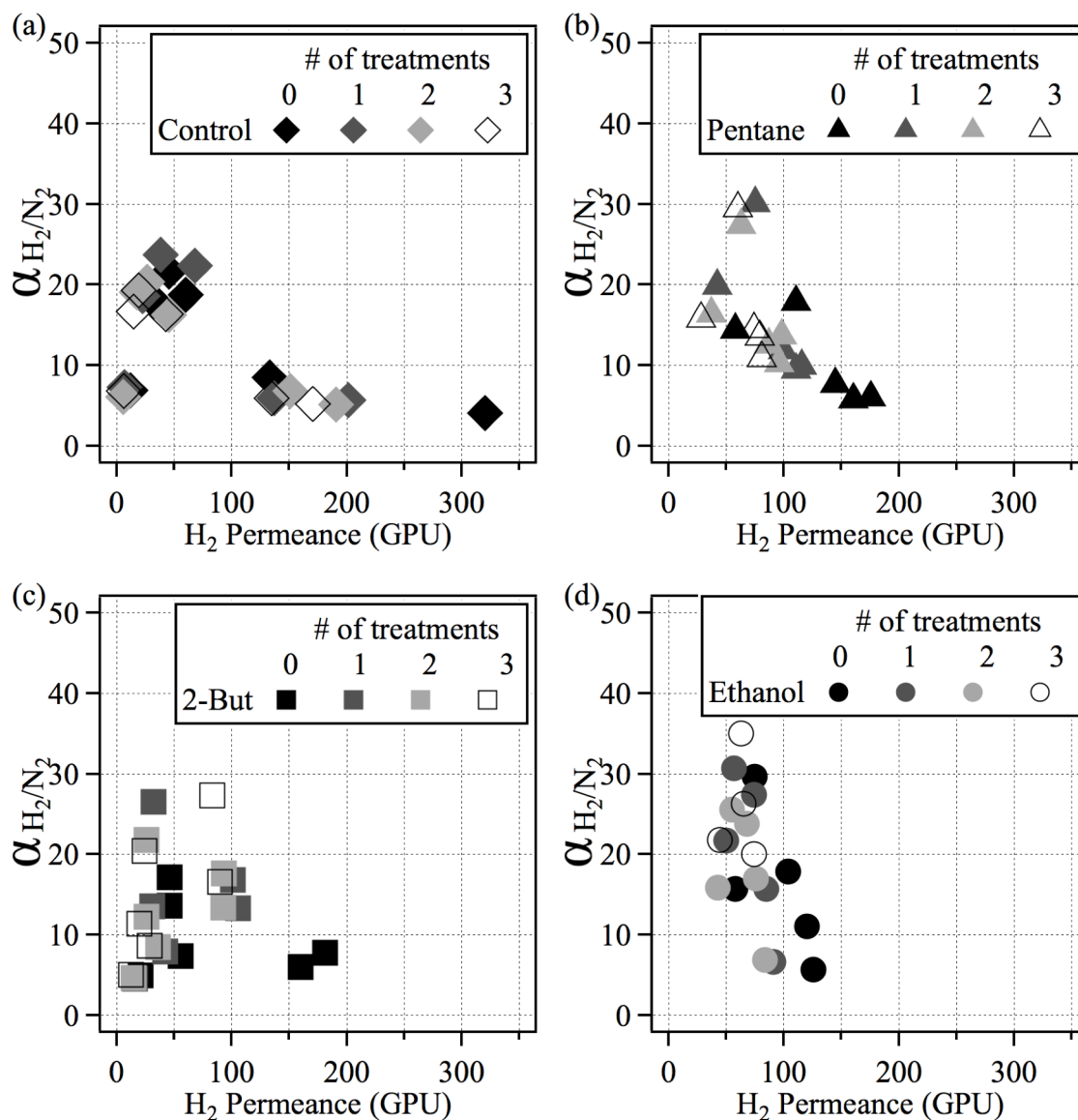


Figure 5–4. Consecutive vapor treatments result in most membranes having lower permeances and selectivities. Control group remains unchanged. Measurement error is the size of the points. (a) Control (b) Pentane (c) 2-butanone (d) Ethanol

In order to elucidate the effect of treatment on change in selectivity, a statistical analysis was performed on the change in selectivity between treatments. Figure 5–5a shows differences in

improvements in selectivities after one treatment. Only the change in selectivity in the pentane group was different than the control group. Pentane, as noted earlier, has very different solubility parameters than either polymer in the blend membranes. It was speculated that pentane would be least likely to swell the membrane and, therefore, not be able to heal defects. The vapor pressure of the treatment compounds can be found in Table 5–2. Pentane has a higher vapor pressure than

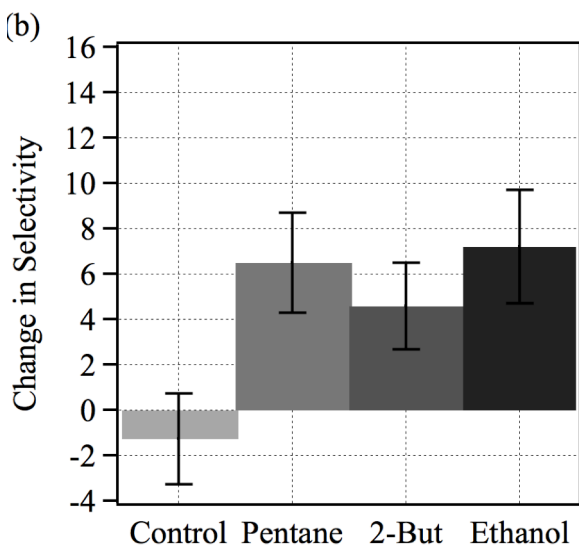
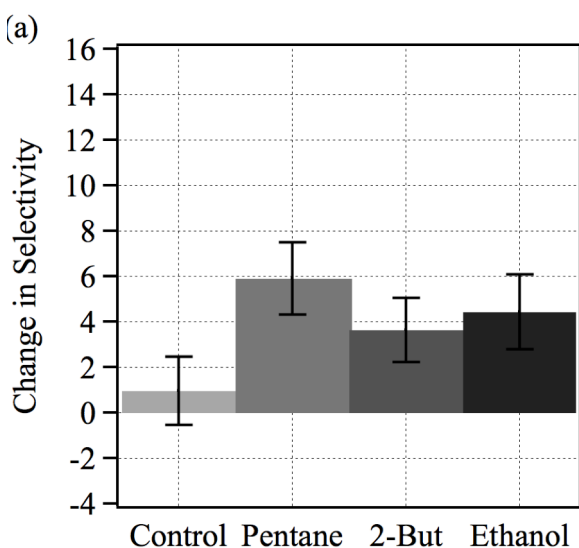


Figure 5–5. Vapor post treatments (a) after one treatment (b) after three treatments. Error bars represent the standard error of the mean change in selectivity.

either 2-butanone or ethanol. The selectivity in the pentane group might be different from the control group, while the same cannot be said for the 2-butanone and ethanol group, because there are enough molecules in the vapor phase to have an effect on the membrane structure.

Figure 5–5b shows the difference in improvements in selectivity after three treatments. After three treatments, all compounds have improved the selectivity of the membranes more than the control, but there is no statistically relevant difference between treatments. There is no difference between improvements in selectivity between one and three treatments of pentane. After a single treatment, no further improvement is realized. In the case of 2-butanone and ethanol, after 90 minutes of treatment there are improvements in selectivity beyond that of the control group. For the group of compounds studied, those with lower vapor pressures require more treatment time to have an effect on selectivity.

Table 5–2. Vapor pressures of chosen post-treatments

Treatment compound	P_{vap} (atm, 25°C)
Pentane	0.621
2-butanone	0.151
Ethanol	0.109

of pentane or 2-butanone. For membranes treated with pentane, those with Knudsen diffusion sized pores did not improve. Some membranes with moderate fluxes between 70 and 150 GPU, and selectivities above 10, were improved by treatment with pentane. For membranes treated with 2-butanone, only the worst membrane with the lowest selectivity was not improved. The result of three consecutive treatments is shown in Figure 5–7. Again, as membranes go through more treatments, the permeances tend to be lower and the selectivities higher.

3.3 Liquid post-treatments

For liquid post-treatments, membranes exposed to ethanol curled and became unusable. For these membranes, ethanol is too strong of an agent for liquid treatments. Figure 5–6 shows the selectivity before and after one liquid treatment

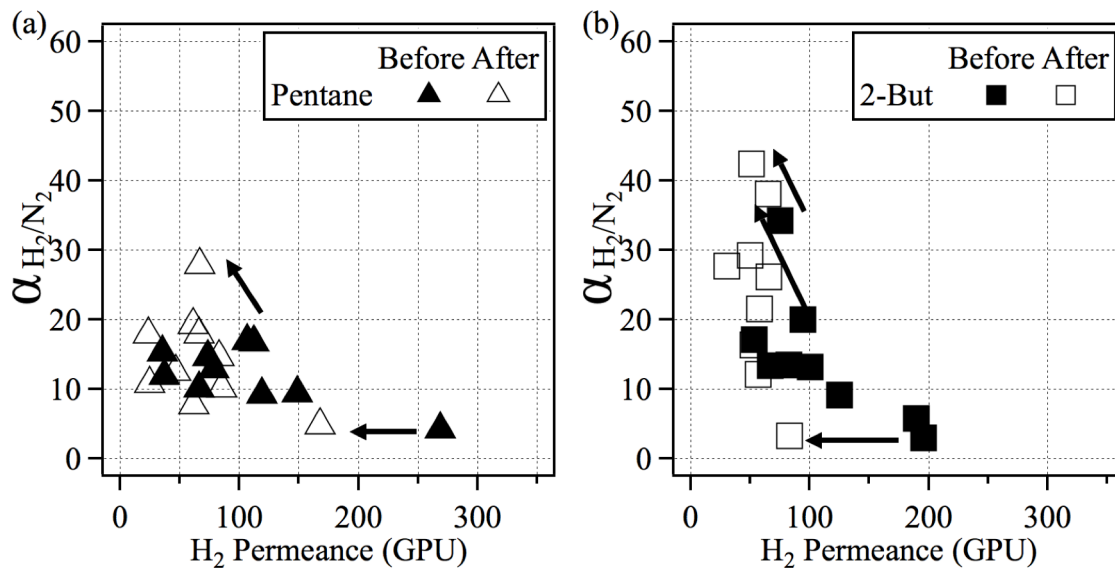


Figure 5–6. After one liquid treatment, only a few membranes in the pentane group improved while almost all membranes in the 2-butanone group improved. Control group is the same as Figure 5–3a. Measurement error is the size of the points. (a) Pentane (b) 2-butanone

Statistical analysis shows after one treatment, there is no difference between the pentane group and the control group (Figure 5–8). There is a significant improvement in selectivity with the group treated with 2-butanone. After three treatments, there is a significant difference

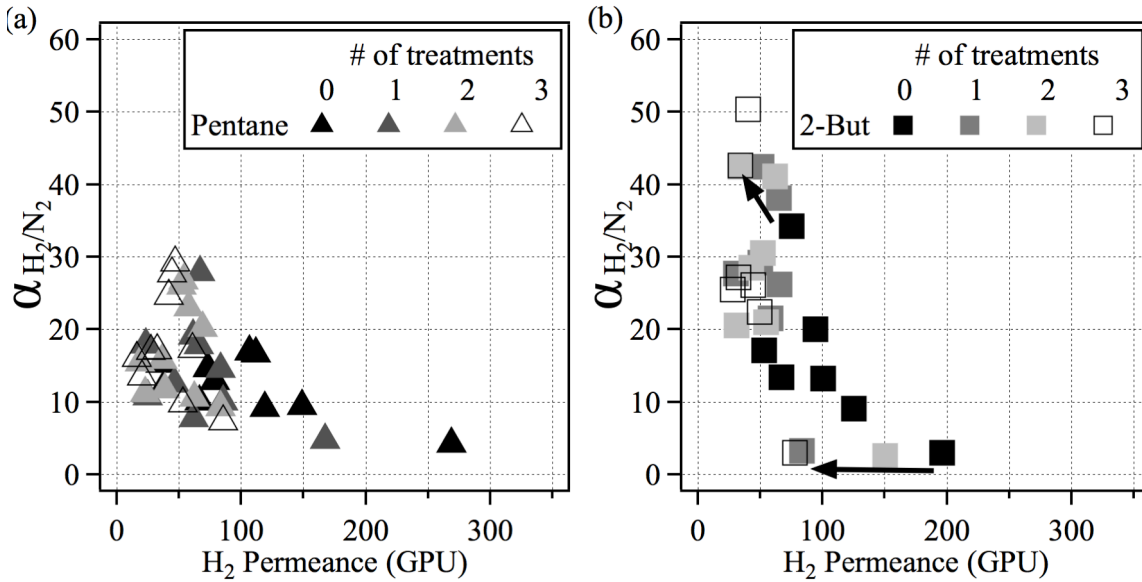


Figure 5–7. Consecutive liquid treatments result most membranes having lower permeances and selectivities. Control group is the same as Figure 5–4a. Measurement error is the size of the points. (a) Pentane (b) 2-butanone

between the control group and both the pentane and 2-butanone group. The 2-butanone group performed better than the pentane group. While pentane continued to improve the selectivity of membranes with successive treatments, the 2-butanone group did not see an improvement in selectivity between the first and third treatment.

Pentane, after three liquid treatments, saw the same improvement as one vapor treatment. Pentane might require fewer vapor treatments because it readily evaporates. It should be noted that for the liquid case, pentane was allowed to remain on the surface for 5 minutes per treatment, with a total of 15 minutes for three treatments, before being placed in the vacuum oven, while for vapor case, the membrane remained exposed to vapor for 30 minutes per treatment, for a total of 90 minutes exposed to the vapor. The amount of contact time was much lower in the case of the liquid treatment, but the improvement was the same. 2-butanone improved the membrane more in the liquid treatment case than in the vapor case. This could be because 2-butanone does not evaporate so readily so the vapor treatment was not as effective, but the liquid treatment was because it stayed on the surface longer.

4. Conclusions

Alkanes, ketones, and alcohols can be used to improve the selectivity of blended PBI-Matrimid membranes with either vapor or liquid treatments. The amount of improvement appears to depend on the chemical nature of the compounds, their physical properties and both the type of treatment and the amount of time spent being treated. The vapor pressure appears to be a critical component in whether a vapor treatment or liquid treatment will have the best effect. Compounds with low vapor pressures might have more improvements in selectivity when used as liquid treatment. Common, benign compounds can be used to improve the selectivity of blended polymeric membranes.

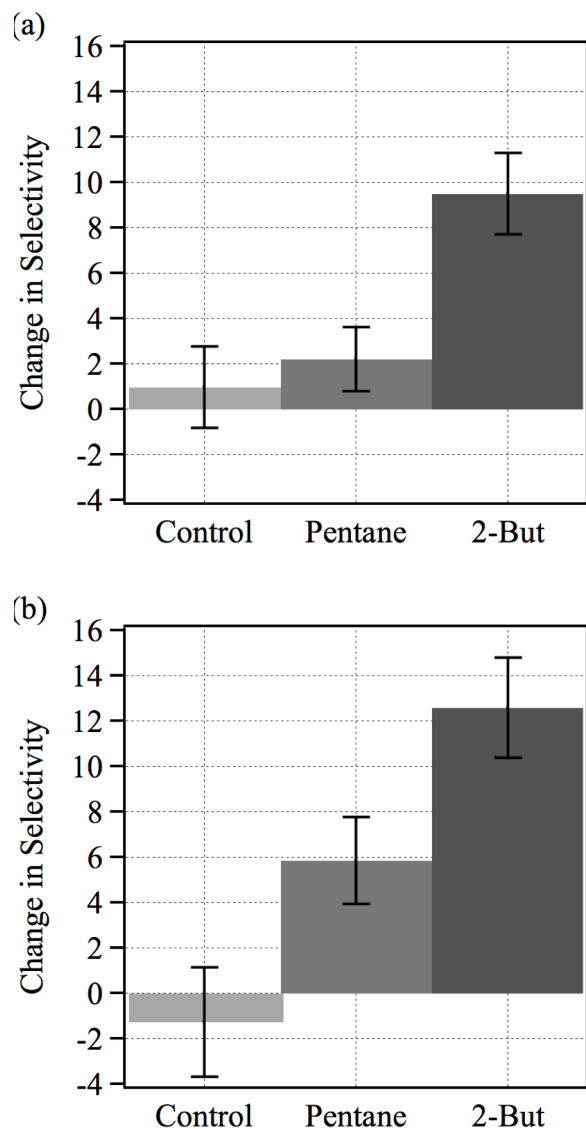


Figure 5–8. Liquid post treatments (a) after one treatment (b) after three treatments. Error bars represent the standard error of the mean change in selectivity.

Chapter 6 - Conclusions and future work

Blended PBI/Matrimid dense films and asymmetric membranes were fabricated and characterized across a range of temperatures. All dense films have less than 1wt% mass loss at 300°C suggesting the materials can operate up to this temperature without thermally decomposing and indeed, 50/50 asymmetric membranes continue to separate gases at this temperature. Asymmetric membranes, with their thin selective skin on a porous substructure, are attractive for separations because they are selective, producing streams enriched in one or more components, while still having large amounts of material pass through them because the selective skin layer is thin. With their significant resistance to chemical attack and ability to separate gaseous components up to 300°C, the blended asymmetric membranes could be used in several applications. These include both separations and reaction applications. The blended membranes could be used in nanofiltration separations, such as those with hot feeds or those containing components typically associated with dissolving or swelling polymers, such as aromatics or highly polar components. High temperature gas separations for environmental applications, such as H₂ recovery in biomass pyrolysis or in low-temperature water-gas shift reactions, would be another possible application. In reactions, there are many equilibrium and three-phase reactions, including dehydrogenation and hydrogenation, both of which are important to the chemical industry and performed at elevated temperatures, which could benefit from the inclusion of an asymmetric membrane for either product separation or as a phase contactor.

It must be noted when these materials are operated at temperatures in excess of 100°C in the asymmetric configuration, the substructure tightens, and gases see resistance to transport in the porous substructure as well as the selective skin layer. This is detrimental to both permeance and selectivity. In the future, high temperature membrane separations would benefit from the development of materials or processes that are able to maintain large pores at elevated temperatures.

Selectivity is a critical property of gas separation membranes. We have shown that a variety of benign compounds can be used to improve selectivity of blended membranes. Factors affecting the improvement in selectivity include whether a vapor or liquid is applied to the surface, as well as the chemical and physical nature of the compound. In liquid separations

where these compounds are already present, improvements in online selectivity are likely to occur.

References

- [1] Materials for Separation Technologies: Energy and Emission Reduction Opportunities, 2005.
- [2] S.S. Hosseini, T.S. Chung, Carbon membranes from blends of PBI and polyimides for N₂/CH₄ and CO₂/CH₄ separation and hydrogen purification, *J. Memb. Sci.* 328 (2009) 174–185. doi:10.1016/j.memsci.2008.12.005.
- [3] R. Baker, *Membrane Technology and Applications*, 3rd ed., John Wiley & Sons, Inc., Chichester, UK, 2012.
- [4] T. Graham, No Title, London, Edinburgh, Dublin Philos. Mag. J. Sci. 32 (1866) 503.
- [5] K. Scott, *Handbook of Industrial Membrane Technology*, 2nd ed., Elsevier Advanced Technology, 1995.
- [6] A. Flint, *The physiology of man*, D. Appleton and Company, New York, 1866.
- [7] J.K. Mitchell, On the penetrativeness of fluids, *Am. J. Med. Sci.* (1830) 36.
- [8] A. Fick, Uber Diffusion, *Poggendorff's Ann. Der Phys. Und Chemie.* 94 (1855) 59.
- [9] T. Graham, On the adsorption and dialytic separation of gases by colloid septa, London, Edinburgh, Dublin Philos. Mag. J. Sci. 32 (1866) 401.
- [10] S. Loeb, S. Sourirajan, Sea water demineralization by means of an osmotic membrane, in: *Adv. Chem. Ser.*, 1963: pp. 117–132.
- [11] J. Henis, M. Tripodi, Composite hollow fiber membranes for gas separation: The resistance model approach, *J. Memb. Sci.* 8 (1981) 233–246.
- [12] J.M.S. Henis, M.K. Tripodi, Multicomponent membranes for gas separations, US Pat. 4,230,463, 1980.
- [13] P. Vandezande, L.E.M. Gevers, I.F.J. Vankelecom, Solvent resistant nanofiltration: separating on a molecular level., *Chem. Soc. Rev.* 37 (2008) 365–405. doi:10.1039/b610848m.
- [14] M. Sairam, X.X. Loh, Y. Bhole, I. Sereewatthanawut, K. Li, a. Bismarck, et al., Spiral-wound polyaniline membrane modules for organic solvent nanofiltration (OSN), *J. Memb. Sci.* 349 (2010) 123–129. doi:10.1016/j.memsci.2009.11.039.
- [15] A. Dobrak, B. Verrecht, H. Van den Dungen, A. Buekenhoudt, I.F.J. Vankelecom, B. Van der Bruggen, Solvent flux behavior and rejection characteristics of hydrophilic and

- hydrophobic mesoporous and microporous TiO₂ and ZrO₂ membranes, *J. Memb. Sci.* 346 (2010) 344–352. doi:10.1016/j.memsci.2009.09.059.
- [16] M. Sairam, X.X. Loh, K. Li, A. Bismarck, J.H.G. Steinke, A.G. Livingston, Nanoporous asymmetric polyaniline films for filtration of organic solvents, *J. Memb. Sci.* 330 (2009) 166–174. doi:10.1016/j.memsci.2008.12.067.
- [17] C. Ba, J. Langer, J. Economy, Chemical modification of P84 copolyimide membranes by polyethylenimine for nanofiltration, *J. Memb. Sci.* 327 (2009) 49–58. doi:10.1016/j.memsci.2008.10.051.
- [18] D. Singh, M.E. Rezac, P.H. Pfromm, Partial Hydrogenation of Soybean Oil with Minimal Trans Fat ..., *J. Am. Oil Chem. Soc.* 86 (2009) 93–101.
- [19] D. Singh, P.H. Pfromm, M.E. Rezac, Overcoming Mass-Transfer Limitations in Partial Hydrogenation of Soybean Oil Using Metal-Decorated Polymeric Membranes, *AIChE J.* 57 (2011). doi:10.1002/aic.
- [20] M.E. Rezac, W.J. Koros, S. Miller, Membrane-assisted dehydrogenation of n-butane; Influence of membrane properties on system performance, *J. Memb. Sci.* 93 (1994) 193–201.
- [21] F. Zhang, M.E. Rezac, S. Majumdar, P. Kosaraju, S. Nemser, Improving chemical production processes by selective by-product removal in a pervaporation membrane reactor, *Sep. Sci. Technol.* 49 (2014) 1289–1297.
- [22] A. Parkes, No Title, British Pat 1,147, 1846.
- [23] S. Basu, A. Cano-Odena, I.F.J. Vankelecom, Asymmetric membrane based on Matrimid® and polysulphone blends for enhanced permeance and stability in binary gas (CO₂/CH₄) mixture separations, *Sep. Purif. Technol.* 75 (2010) 15–21. doi:10.1016/j.seppur.2010.07.004.
- [24] M.M. Teoh, T.-S. Chung, K.Y. Wang, M.D. Guiver, Exploring Torlon/P84 co-polyamide-imide blended hollow fibers and their chemical cross-linking modifications for pervaporation dehydration of isopropanol, *Sep. Purif. Technol.* 61 (2008) 404–413. doi:10.1016/j.seppur.2007.12.002.
- [25] M.E. Rezac, B. Schoberl, Transport and thermal properties of poly(ether imide)/acetylene-terminated monomer blends, *J. Memb. Sci.* 156 (1999) 1999.

- [26] N. Muruganandam, D.R. Paul, Evaluation of substituted polycarbonates and a blend with polystyrene as gas separation membranes, *J. Memb. Sci.* 34 (1987) 185–198.
- [27] R.M. Barrer, *Diffusion in and through solids*, Cambridge Press, London, 1951.
- [28] L.M. Costello, W.J. Koros, Thermally stable polyimide isomers for membrane-based gas separations at elevated temperatures, *J. Polym. Sci. Part B Polym. Phys.* 33 (1995) 135–146.
- [29] J.G. Kirkwood, I. Oppenheim, *Chemical Thermodynamics*, McGraw-Hill, New York, 1961.
- [30] L.M. Robeson, The upper bound revisited, *J. Memb. Sci.* 320 (2008) 390–400.
<http://linkinghub.elsevier.com/retrieve/pii/S0376738808003347> (accessed April 28, 2014).
- [31] A. Car, C. Stropnik, W. Yave, K.-V. Peinemann, Pebax®/polyethylene glycol blend thin film composite membranes for CO₂ separation: Performance with mixed gases, *Sep. Purif. Technol.* 62 (2008) 110–117.
<http://linkinghub.elsevier.com/retrieve/pii/S1383586608000142> (accessed April 19, 2014).
- [32] G.C. Kapantaidakis, S.P. Kaldis, X.S. Dabou, G.P. Sakellaropoulos, Gas permeation through PSF-PI miscible blend membranes, *J. Memb. Sci.* 110 (1996) 239–247.
- [33] J.C. Jansen, S. Darvishmanesh, F. Tasselli, F. Bazzarelli, P. Bernardo, E. Tocci, et al., Influence of the blend composition on the properties and separation performance of novel solvent resistant polyphenylsulfone/polyimide nanofiltration membranes, *J. Memb. Sci.* 447 (2013) 107–118. doi:10.1016/j.memsci.2013.07.009.
- [34] D.Y. Xing, S.Y. Chan, T.-S. Chung, Fabrication of porous and interconnected PBI/P84 ultrafiltration membranes using [EMIM]OAc as the green solvent, *Chem. Eng. Sci.* 87 (2013) 194–203. doi:10.1016/j.ces.2012.10.004.
- [35] O. Olabisi, A.G. Farnham, *Polymer Compatibilization: Blends of Polyarylethers with Styrenic Interpolymers*, in: *Adv. Chem. Ser.*, 1979: pp. 559–585.
- [36] Y. Maeda, D.R. Paul, Selective gas transport in miscible PPO-PS blends, *Polymer (Guildf)*. 26 (1985) 2055–2063.
- [37] A. Parkes, Preparation of certain vegetable and animal substances and certain combinations of the same substances alone or with other substances, *British Pat* 11,147, 1846.

- [38] M. Wessling, M. Lidon Lopez, H. Strathmann, Accelerated plasticization of thin-film composite membranes used in gas separation, *Sep. Purif. Technol.* 24 (2001) 223–233. doi:10.1016/S1383-5866(01)00127-7.
- [39] S. Shishatskiy, C. Nistor, M. Popa, S.P. Nunes, K. V. Peinemann, Polyimide asymmetric membranes for hydrogen separation: Influence of formation conditions on gas transport properties, *Adv. Eng. Mater.* 8 (2006) 390–397. doi:10.1002/adem.200600024.
- [40] O.C. David, D. Gorri, A. Urriaga, I. Ortiz, Mixed gas separation study for the hydrogen recovery from H₂/CO/N₂/CO₂ post combustion mixtures using a Matrimid membrane, *J. Memb. Sci.* 378 (2011) 359–368. doi:10.1016/j.memsci.2011.05.029.
- [41] D. Clausi, W. Koros, Formation of defect-free polyimide hollow fiber membranes for gas separations, *J. Memb. Sci.* 167 (2001) 79–89.
- [42] H.-Y. Zhao, Y.-M. Cao, X.-L. Ding, M.-Q. Zhou, Q. Yuan, Effects of cross-linkers with different molecular weights in cross-linked Matrimid 5218 and test temperature on gas transport properties, *J. Memb. Sci.* 323 (2008) 176–184. doi:10.1016/j.memsci.2008.06.026.
- [43] J.R. Klaehn, T.A. Luther, C.J. Orme, M.G. Jones, A.K. Wertsching, E.S. Peterson, New soluble n-substituted polybenzimidazole by post-polymerization modification, *Polym. Prepr.* 46 (2005) 708–709.
- [44] T.-S. Chung, W.F. Guo, Y. Liu, Enhanced Matrimid membranes for pervaporation by homogenous blends with polybenzimidazole (PBI), *J. Memb. Sci.* 271 (2006) 221–231. doi:10.1016/j.memsci.2005.07.042.
- [45] G. Kung, L.Y. Jiang, Y. Wang, T.-S. Chung, Asymmetric hollow fibers by polyimide and polybenzimidazole blends for toluene/iso-octane separation, *J. Memb. Sci.* 360 (2010) 303–314. doi:10.1016/j.memsci.2010.05.030.
- [46] S. Hosseini, T.-S. Chung, Polymer blends and carbonized polymer blends, US Pat. 13/122,843, 2011.
- [47] S.S. Hosseini, M.M. Teoh, T.S. Chung, Hydrogen separation and purification in membranes of miscible polymer blends with interpenetration networks, *Polymer (Guildf)*. 49 (2008) 1594–1603. doi:10.1016/j.polymer.2008.01.052.
- [48] S.S. Hosseini, N. Peng, T.S. Chung, Gas separation membranes developed through integration of polymer blending and dual-layer hollow fiber spinning process for hydrogen

- and natural gas enrichments, *J. Memb. Sci.* 349 (2010) 156–166.
doi:10.1016/j.memsci.2009.11.043.
- [49] L.M. Costello, W.J. Koros, Temperature dependence of gas sorption and transport properties in polymers: measurement and applications, *Ind. Eng. Chem. Res.* 31 (1992) 2708–2714. <http://pubs.acs.org/doi/abs/10.1021/ie00012a012>.
- [50] H. Czichos, T. Saito, L. Smith, eds., *Springer Handbook of Materials Measurement Methods*, Springer Berlin Heidelberg, 2006.
- [51] J.M. Brown, B.M. Kadlubowski, L.J. Forney, J.T. Sommerfeld, Density gradient columns: Dynamic modeling for linear profiles, *Rev. Sci. Instrum.* 67 (1996) 3973–3980.
<http://scitation.aip.org/content/aip/journal/rsi/67/11/10.1063/1.1147301> (accessed April 12, 2014).
- [52] M.E. Rezac, E. Todd Sorensen, H.W. Beckham, Transport properties of crosslinkable polyimide blends, *J. Memb. Sci.* 136 (1997) 249–259.
- [53] R.E. Kesting, A.K. Fritzsche, *Polymeric gas separation membranes*, John Wiley & Sons, Inc., New York, 1993.
- [54] M.E. Rezac, P.H. Pfromm, L.M. Costello, W.J. Koros, Aging of thin polyimide-ceramic and polycarbonate-ceramic composite membranes, *Ind. Eng. Chem. Res.* 32 (1993) 1921–1926.
- [55] S. Qiu, *Preparation and characterization of Matrimid/P84 Blend Films*, Kansas State University, 2015.
- [56] D.W. van Krevelen, K. te Nijenhuis, *Properties of polymers*, 4th ed., Elsevier B.V., Amsterdam, 2009.
- [57] T.D. Dang, L.S. Tan, F.E. Arnold, Benzimidazole pendant rigid-rod benzobisthiazole polymers, *Polym. Prepr.* 31 (1990) 451.
- [58] R.-C. Ruaan, T.-H. Wu, S.-H. Chen, J.-Y. Lai, Oxygen/nitrogen separation by polybutadine/polycarbonate composite membranes modified by ethylenediamine plasma, *J. Memb. Sci.* 138 (1998) 213–220.
- [59] A.B. Conciatori, E.C. Chenevey, T.C. Bohrer, A.E. Prince Jr., Polymerization and spinning of PBI, *J. Polym. Sci. Part C.* 19 (1967) 49–64.
- [60] I. Pinnau, *Skin formation of integral-asymmetric gas separation membranes made by dry/wet phase inversion*, University of Texas at Austin, 1991.

- [61] H. Strathmann, K. Kock, P. Amar, R.W. Baker, The formation mechanism of asymmetric membranes, *Desalination*. 16 (1975) 179–203.
- [62] K.A. Berchtold, R.P. Singh, J.S. Young, K.W. Dudeck, Polybenzimidazole composite membranes for high temperature synthesis gas separations, *J. Memb. Sci.* 415-416 (2012) 265–270. <http://linkinghub.elsevier.com/retrieve/pii/S0376738812003699> (accessed April 12, 2014).
- [63] J. Albo, J. Wang, T. Tsuru, Application of interfacially polymerized polyamide composite membranes to isopropanol dehydration: Effect of membrane pre-treatment and temperature, *J. Memb. Sci.* 453 (2014) 384–393. doi:10.1016/j.memsci.2013.11.030.
- [64] W.J. Koros, D.G. Woods, Elevated temperature application of polymer hollow-fiber membranes, *J. Memb. Sci.* 181 (2001) 157–166.
- [65] Costello, Walker, Koros - 1994 - Analysis of a thermally stable polypyrrolone for high temp membrane-based GS.pdf, (n.d.).
- [66] T.-S. Chung, W. Guo, Y. Liu, Enhanced Matrimid membranes for pervaporation by homogeneous blends with polybenzimidazole (PBI), *J. Memb. Sci.* 271 (2006) 221–231.
- [67] S. Hosseini, M. Teoh, Chung, Hydrogen separation and purification in membranes of miscible polymer blend with interpenetration networks, *Polymer (Guildf)*. 49 (2008) 1594–1603.
- [68] M.E. Rezac, N.S. Moore, A. Back, Effect of temperature on the transport properties and morphology of polymeric asymmetric membranes, *Sep. Sci. Technol.* 32 (1997) 505–525.
- [69] I. Pinnau, W.J. Koros, Relationship between Substructure Resistance and Gas Separation Properties of Defect-Free Integrally Skinned Asymmetric Membranes, *Ind. Eng. Chem. Res.* 30 (1991) 1837–1840.
- [70] K.K. Hsu, S. Nataraj, R.M. Thorogood, P.S. Puri, O₂/N₂ Selectivity improvement for polytrimethylsilylpropyne membranes by UV-irradiation and further enhancement by subambient temperature operation, *J. Memb. Sci.* 79 (1993) 1–10.
- [71] S.M. Mahurin, J.S. Lee, X. Wang, S. Dai, Ammonia-activated mesoporous carbon membranes for gas separations, *J. Memb. Sci.* 368 (2011) 41–47. doi:10.1016/j.memsci.2010.11.007.
- [72] J.M. Mohr, D.R. Paul, I. Pinnau, W.J. Koros, Surface fluorination of polysulfone asymmetric membranes and films, *J. Memb. Sci.* 56 (1991) 77–98.

- [73] S.-H. Choi, M.-K. Lee, S.-J. Oh, J.-K. Koo, Gas sorption and transport of ozone-treated polysulfone, *J. Memb. Sci.* 221 (2003) 37–46. doi:10.1016/S0376-7388(03)00081-4.
- [74] B. Cai, In situ reparation of defects on the skin layer of reverse osmosis cellulose ester membranes for pervaporation purposes, *J. Memb. Sci.* 216 (2003) 165–175. doi:10.1016/S0376-7388(03)00068-1.
- [75] J. Louie, I. Pinnau, M. Reinhard, Gas and liquid permeation properties of modified interfacial composite reverse osmosis membranes, *J. Memb. Sci.* 325 (2008) 793–800. doi:10.1016/j.memsci.2008.09.006.
- [76] I. Pinnau, J. Wind, Process for increasing the selectivity of asymmetric membranes, US Pat. 5,007,944, 1991.
- [77] M.E. Rezac, J.D. Le Roux, H. Chen, D.R. Paul, W.J. Koros, Effect of mild solvent post-treatments on the gas transport properties of glassy polymer membranes, *J. Memb. Sci.* 90 (1994) 213–229.
- [78] A. Wolinska-Grabczyk, Transport of liquid hydrocarbons in the polyurethane-based membranes, *J. Memb. Sci.* 302 (2007) 59–69.
- [79] B. Shi, C. Feng, Y. Wu, A new method of measuring alcohol clusters in polyimide membrane : combination of inverse gas chromatography with equilibrium swelling, 245 (2004) 87–93. doi:10.1016/j.memsci.2004.08.003.
- [80] K. Friess, Comparison of permeability coefficients of organic vapors through non-porous polymer membranes by two different experimental techniques, *J. Memb. Sci.* 240 (2004) 179–185. doi:10.1016/j.memsci.2004.05.006.
- [81] M. Dingemans, J. Dewulf, A. Kumar, H. Van Langenhove, Solubility of volatile organic compounds in polymers: Effect of polymer type and processing, *J. Memb. Sci.* 312 (2008) 107–114. doi:10.1016/j.memsci.2007.12.042.
- [82] C.M. Hansen, Hansen solubility parameters: a user's handbook, CRC Press, Inc, Boca Raton, FL, 2000.
- [83] J.H. Hildebrand, Factors determining solubility among non-electrolytes, *Proc. Natl. Acad. Sci. U. S. A.* 36 (1950) 7–15.
- [84] G.Q. Chen, C.A. Scholes, C.M. Doherty, A.J. Hill, G.G. Qiao, S.E. Kentish, The thickness dependence of Matrimid films in water vapor permeation, *Chem. Eng. J.* 209 (2012) 301–312. doi:10.1016/j.cej.2012.07.135.

- [85] B. Schoberl, Temperatureinfluss auf polymermembranen, 1997.
- [86] E. V Perez, K.J. Balkus Jr., J.P. Ferraris, I.H. Musselman, Metal-organic polyhedra 18 mixed-matrix membranes for gas separation, *J. Memb. Sci.* 463 (2014) 82–93. doi:10.1016/j.memsci.2014.03.045.
- [87] Y. Zhang, I.H. Musselman, J.P. Ferraris, K.J.B. Jr, Gas permeability properties of Matrimid® membranes containing the metal-organic framework Cu–BPY–HFS, *J. Memb. Sci.* 313 (2008) 170–181. doi:10.1016/j.memsci.2008.01.005.
- [88] H.-W. Rösler, Membrantechnologie in der Prozessindustrie - Polymere Membranwerkstoffe, *Chemie Ing. Tech.* 77 (2005) 487–503. doi:10.1002/cite.200500031.
- [89] M.J.C. Ordoñez, K.J. Balkus, J.P. Ferraris, I.H. Musselman, Molecular sieving realized with ZIF-8/Matrimid® mixed-matrix membranes, *J. Memb. Sci.* 361 (2010) 28–37. doi:10.1016/j.memsci.2010.06.017.
- [90] D.R. Pesiri, B. Jorgensen, R.C. Dye, Thermal optimization of polybenzimidazole meniscus membranes for the separation of hydrogen, methane, and carbon dioxide, *J. Memb. Sci.* 218 (2003) 11–18. doi:10.1016/S0376-7388(03)00129-7.
- [91] S.C. Kumbharkar, M.N. Islam, R.A. Potrekar, U.K. Kharul, Variation in acid moiety of polybenzimidazoles: Investigation of physico-chemical properties towards their applicability as proton exchange and gas separation membrane materials, *Polymer (Guildf)*. 50 (2009) 1403–1413. doi:10.1016/j.polymer.2009.01.043.
- [92] S.C. Kumbharkar, P.B. Karadkar, U.K. Kharul, Enhancement of gas permeation properties of polybenzimidazoles by systematic structure architecture, *J. Memb. Sci.* 286 (2006) 161–169. doi:10.1016/j.memsci.2006.09.030.

Appendix A - Dynamic Mechanical Analysis Data

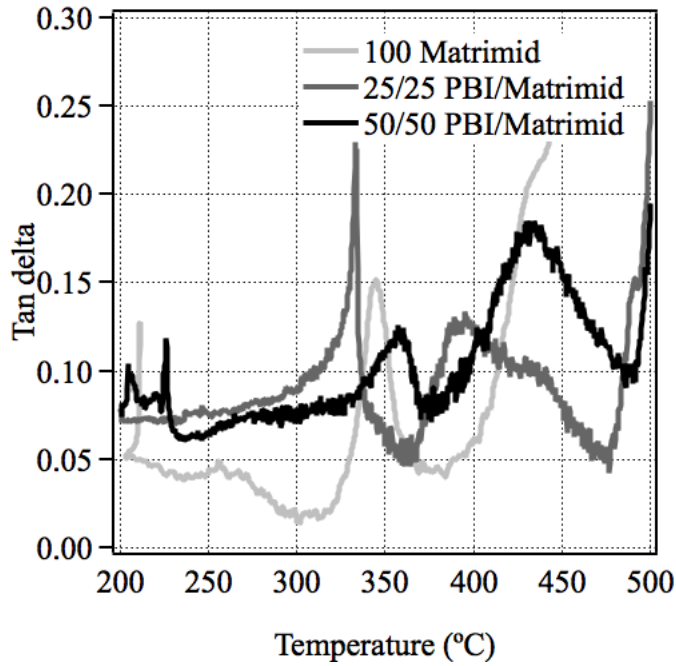


Figure A-1. Tan delta curves show that 25wt% and 50wt% PBI in Matrimid form immiscible blends